AN ALGEBRAIC REPRESENTATION FOR THE TOPOLOGY OF MULTICOMPONENT PHASE DIAGRAMS

Don J. Orser

Center for Manufacturing Engineering
National Bureau of Standards
Gaithersburg, Md 20899

ABSTRACT

A new non-graphical method for representing the topology of phase diagrams is presented. The method exploits the fact that the topological relations between the variously dimensioned equilibria making up the structure of a phase diagram may be treated as a special type of algebraic structure, called an incidence lattice. Corresponding to each topologically distinct phase diagram there is a finite incidence lattice whose elements correspond to the invariant (vertices), monovariant (edges), bivariant (surfaces), etc., transition equilibria of the diagram, and whose operations correspond to moving between these topological elements in a systematic way. Further, we have discovered a method of modeling a given incidence lattice by a family of sets. In this incidence calculus, as we call such a family of sets, the two operations for the incidence lattice are modeled by set intersections. This defines a "calculus" of phase diagram equilibria specific to that diagram and provides an efficient method for a computer to store and subsequently retrieve the topological relationships between an equilibrium and the rest of the diagram or between any two equilibria. A remarkable mathematical fact is that the incidence calculus may be generated from certain subsets of itself. This is reflective of the fact that knowing a "sufficient" portion of the topology uniquely determines the remainder. An algorithm exploiting this fact, based on knowing just which n-dimensional phase fields of an n-ary phase diagram are incident on each vertex (point with zero degrees of freedom), is described. Hence, the higher the dimensionality of the diagram, the higher the return from the algorithm. The application of the incidence calculus to a multicomponent data base and its potential for qualitative thermodynamic modeling are discussed.

February 21, 1986

D. J. Orser, "An Algebraic Representation for the Topology of Multicomponent Phase Diagrams," Proceedings of the Symposium on Computer Modeling of Phase Diagrams, Oct 13-17, 1985, Toronto, Canada, edited by Larry Bennett and published by The Metalurgical Society of AIME, Wallingdale, Pa., 1986.

AN ALGEBRAIC REPRESENTATION FOR THE TOPOLOGY OF MULTICOMPONENT PHASE DIAGRAMS

Don J. Orser

Center for Manufacturing Engineering
National Bureau of Standards
Gaithersburg, Md 20899

1. INTRODUCTION

A phase diagram[1,2] is usually communicated as a pictorial object (figures 5,6 and 8) among human viewers. Presented with such a diagram, a trained human must interpret what he sees in order to make the information contained in the figure explicit within his mind. This process of visual interpretation as performed by a human viewer is not well understood[3] and subsequently not very well emulated by computer. However, the information contained in a phase diagram exists independently of an implicit graphical rendering and for purposes of computer representation, in support of a computerized data base, invites explicit representations which do not require this interpretive step.

In this paper we are concerned with the computer representation of the topological structures inherent in (primarily, temperature-composition) phase diagrams. We advocate the view that these structures must be explicitly represented in the computer in order to easily answer queries regarding phase adjacencies, and present one method of doing so. We will not be concerned with thermodynamic modeling as such, but rather with the representation mathematics useful in understanding how to store the results of such modeling in the computer.

The practical representational problems motivating these ideas are:

(1) Entry Problem: How to enter into the computer higher dimensional phase diagrams.

(2) Subsystem Problem: How to utilize lower order phase diagrams in support of higher order systems within a computerized data base.

(3) Equilibria Adjacency Problem: How to represent the invariant (point), monovariant (boundary), bivariant (surface) etc. transition equilibria in a manner which allows questions concerning their adjacency relationships to be easily answered by computer.

The results we have obtained are due to separating the geometry of a phase diagram into two types of information: the topological and the metrical[4,5], and the realization that the topological information, from a computer representation point of view, is dominant over the metrical, i. e., the metrical information is viewed as attributes of the topological elements. Thus a vertex, a topological object, becomes a geometric point when its temperature-composition coordinate is assigned i.e., the assigning of a metric attribute. In an analogous way edges and faces may be turned into boundaries and surfaces. In this paper we describe a representation for the topological structures making up a phase diagram and for the relations existing between a phase diagram and its subsystems.

Without defining precisely how we distinguish between topological and metrical information, we will use the term *f-equilibria* , $f = 0,1,2, \cdots$, to refer to any equilibrium interface having f degrees of freedom. While not precisely true of all topological elements making up a phase diagram (e.g., a binary eutectic tie-line is not a true *f-equilibria*), we will for the moment use the term vertex for invariant equilibria (0-degrees of freedom), edge for monovariant equilibria (1-degree of freedom), face for bivariant equilibria (2-degrees of freedom) etc., and refer to them in general as *f-equilibria*.

2. PHASE DIAGRAM REPRESENTATION PROBLEM

Consider the problem of entering and representing within the computer a phase diagram such as the ternary diagram depicted at the top of figure 1, in such a way as to facilitate the answering by computer, questions of the following type:

(1) For a given surface, what are its edges?

(2) For a given surface, what volume(s) does it bound?

(3) Given two surfaces, which common volume, if any, is bounded by both?

(4) Given two surfaces, which edges and/or vertices, if any, do they have in common?

(5) Questions (1) - (4) restricted to the binary subsystems.

These questions, asked of a human viewer are easily answered through the process of visual interpretation, but not as easily answered by computer.

If metrical information for individual *f-equilibria*, i.e., phase boundary points, are stored in the computer, then the diagram can be reproduced graphically. However, the information that two *1-equilibria* meet at a eutectic in a binary, for example, is not explicitly known (unless a calculation is performed), and exists only in the mind of the human interpreter as he views the graphical rendering.

One solution is to store tables in the computer containing the precomputed answers and subsequently look up the explicit relationships between a *f-equilibria* and the remaining diagram or between any two *f-equilibria*. Such tables are called incidence matrices[5], and for the ternary of figure 1, characterize the topological relationships between the (for this example) 70 distinct volumes, surfaces, edges and vertices. A disadvantage of this method lies in the amount of work required to generate such tables, and the space required to store them.

We present here an alternative to the above method in the form of a finite mathematical lattice, or lattice algebra[6], specific to the topology of the transition equilibria of a given n-ary phase diagram. The lattice contains as many elements as there are topological elements in the phase diagram. Questions of type (1) - (4) are readily answerable by applying the operations of the lattice to the elements in question, mapping them to the element(s) constituting the answer. Furthermore, we have discovered a simple algorithm for automatically generating the elements of this lattice from information which is readily obtained by visual inspection of a rough drawing or potentially from thermodynamic modeling.

3. TOPOLOGICAL DECOMPOSITION OF A PHASE DIAGRAM

Below the ternary of figure 1 we have depicted its topological decomposition into a hierarchy of volumes, surfaces, edges and vertices. (Only a small subset is actually depicted and the $L+\alpha+\beta$ phase field is left out entirely to simplify the figure.) The relationships asked for by questions (1) - (5) are implicitly represented in this decomposition by the lines connecting the various topological elements and may be easily read off the figure. The trick is to get such a decomposition figure into the computer in a simple way.

To be more precise, we introduce some notation denoting the relations between the topological structures (*f-equilibria*) in the topological decomposition of a phase diagram.

An edge e is said to be a substructure of the surface s which it (partially) bounds. This relationship is indicated by $e < s$ and is read "e is a substructure of s". Conversely, s is a suprastructure of e, and this is indicated by $s > e$. In figure 1, the lines connect just those elements which have this relationship. Questions of type (1) and (2) above are then a matter of finding all elements x which, for a given surface s, satisfy $x < s$ and $s < x$ respectively.

For two distinct surfaces s_1 and s_2 and a volume v, in case both $s_1 < v$ and $s_2 < v$, we say v is the join of s_1 and s_2 and indicate this by $s_1 \uparrow s_2 = v$. Hence, questions of type (3) are a matter of finding, for the given surfaces s_1 and s_2, an x such that $s_1 < x$ and $s_2 < x$.

Similiarly, for surfaces s_1 and s_2 and an edge e, in case $e < s_1$ and $e < s_2$, we say e is the meet of s_1 and s_2 and indicate this by $s_1 \downarrow s_2 = e$. Questions of type (4) are then answered by finding an x such that $x < s_1$ and $x < s_2$ for the two given surfaces s_1 and s_2.

Figure 1 is then a graphical depiction of the *f-equilibria* decomposed into their topological elements in which the substructure relation $<$ is indicated by lines extending down from an element to its substructure elements. In addition, the join $\uparrow$ and meet $\downarrow$ are indicated when two elements have a common suprastructure or substructure respectively.

The explicit representation of the relationships between the topological elements of a phase diagram may be encoded as a list data structure[7], but this still requires that it all be generated in some way. An alternative to such an encoding, we are suggesting, is a lattice modeling the structural relationships between the *f-equilibria*. In this paper we describe such a lattice, in which the join $\uparrow$ and

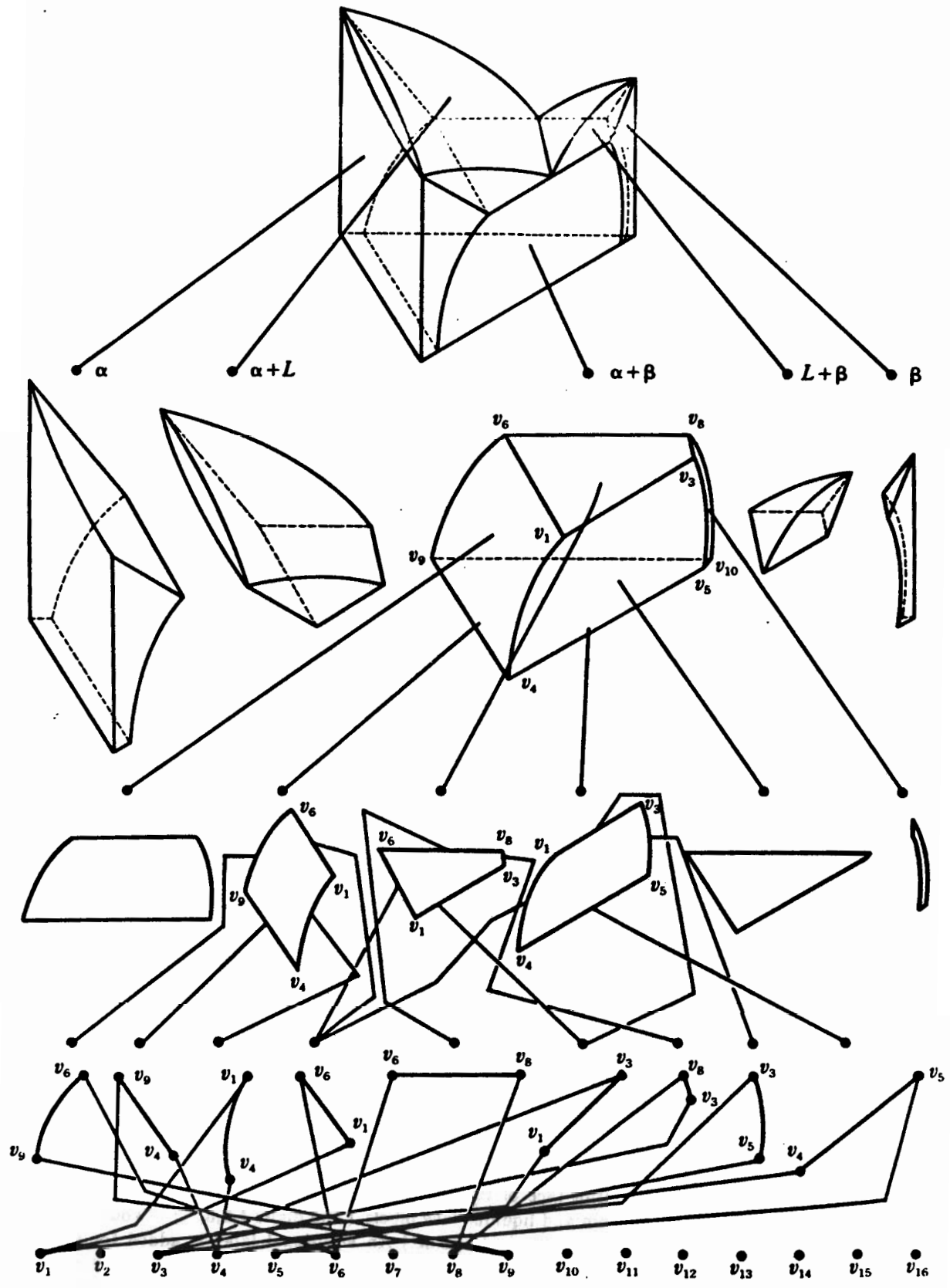

Figure 1. The topological decomposition of a simple ternary. Only the $\alpha + \beta$ phase field is decomposed and the $L + \alpha + \beta$ is left out entirely to simplify the figure. The actual decomposition contains 70 topological elements.

meet $\downarrow$ are implemented by set operations acting on elements of the lattice. Further, we describe a method for computing all the elements of the lattice for a n-ary phase diagram from a knowledge of just the substructure $<$ relationship between the *0-equlibria* and the *n-equilibria*.

In order to differentiate between *f-equilibria* and the topological structures representing them in a phase diagram, we introduce the term *k-face* to refer to a topological element of dimension k. Hence *0-faces* are vertices, *1-faces* edges, *2-faces* surfaces and *3-faces* volumes. We will use *i-face*, *j-face*, *k-face*, $\cdots$ to refer to topological elements of dimension $i, j, k, \cdots$. By referring to a given topological element as a *k-face*, we emphasize its topological dimension k, while referring to it as an *f-equilibrium*, we empasize its associated degrees of freedom f. Note that for a fixed *f-equilibrium*, referred to also as a *k-face*, $f \leq k$, and in particuliar, for a binary eutectic tie-line, for example, $f=0<1=k$.

Using this notation we may summarize the above definitions for the substructure relation and the join and meet operations between the topological elements representing the *f-equilibria* of a n-ary phase diagram, generalized to *k-faces* and also allowing a *k-face* to be a substructure of itself, $0 \leq i, j, k \leq n$ by:

$$i\text{-face} \leq j\text{-face} \text{ if and only if } \begin{cases} i \leq j \\ i\text{-face is a substructure of } j\text{-face} \\ j\text{-face is a suprastructure of } i\text{-face} \end{cases}$$

$$i\text{-face} \uparrow j\text{-face} = k\text{-face} \text{ if and only if } \begin{cases} k \geq max(i,j) \\ k\text{-face} \geq i\text{-face} \\ k\text{-face} \geq j\text{-face} \\ k \text{ is minimum (element of lowest dimension)} \end{cases}$$

$$i\text{-face} \downarrow j\text{-face} = k\text{-face} \text{ if and only if } \begin{cases} k \leq min(i,j) \\ k\text{-face} \leq i\text{-face} \\ k\text{-face} \leq j\text{-face} \\ k \text{ is maximum (element of highest dimension)} \end{cases}$$

4. AN EXAMPLE LATTICE CALCULUS

In order to simplify the presentation given here, we will exemplify our ideas in terms of a much simpler "phase diagram", namely the one shown in figure 2, which we shall refer to as P[A,B,C]. We write it this way to emphasize that three of the faces of the ternary prism are the binary subsytems P[A,B], P[B,C] and P[C,A]. There are two volumes (the interior of the figure and the exterior), five faces, nine edges and six vertices, making a total of 22 *k-faces*, $k=0,1,2,3$, which agrees with Eulers well known identity[8] $vertices - edges + faces - volumes = 6-9+5-2=0$.

We enumerate the lattice elements of the proposed lattice for representing P[A,B,C] in table I, under the column labeled "Incidence Set". Their individual identification with the *k-faces* of P[A,B,C] are enumerated in the third column, while the first column name will be used in the text. For the moment, ignore column four.

Each lattice element consists of a set of labels taken from the set {A-B,B-C,C-A,-B,-L,α}, which we will refer to as the label set for P[A,B,C]. The label set is generated by assigning a unique label to each "region" incident on an exterior face of P[A,B,C], so that A-B,B-C,C-A are the binary subsystem labels, and -B and -L are the bottom and liquidus face labels. (The digits 1,2,3, $\cdots$ would serve as well, but we will use labels which have a mnemonic value.) An additional label is added for each interior phase field. In the case of P[A,B,C], there is only one, which we have labeled α. The "-", when used in a label, mnemonically indicates an exterior face label, as opposed to an interior phase field, where conventional phase field labels will be used.

Each lattice element, or incidence set as we shall refer to them, may be thought of in the following way: For the topological element it corresponds to, it is the set of labels corresponding to the volumes (*n-faces* for a n-ary phase diagram), which are incident to (i.e., touch) that element. For example the "regions" labeled A-B,-B, and α are all incident on the edge e_{12} and hence the lattice element

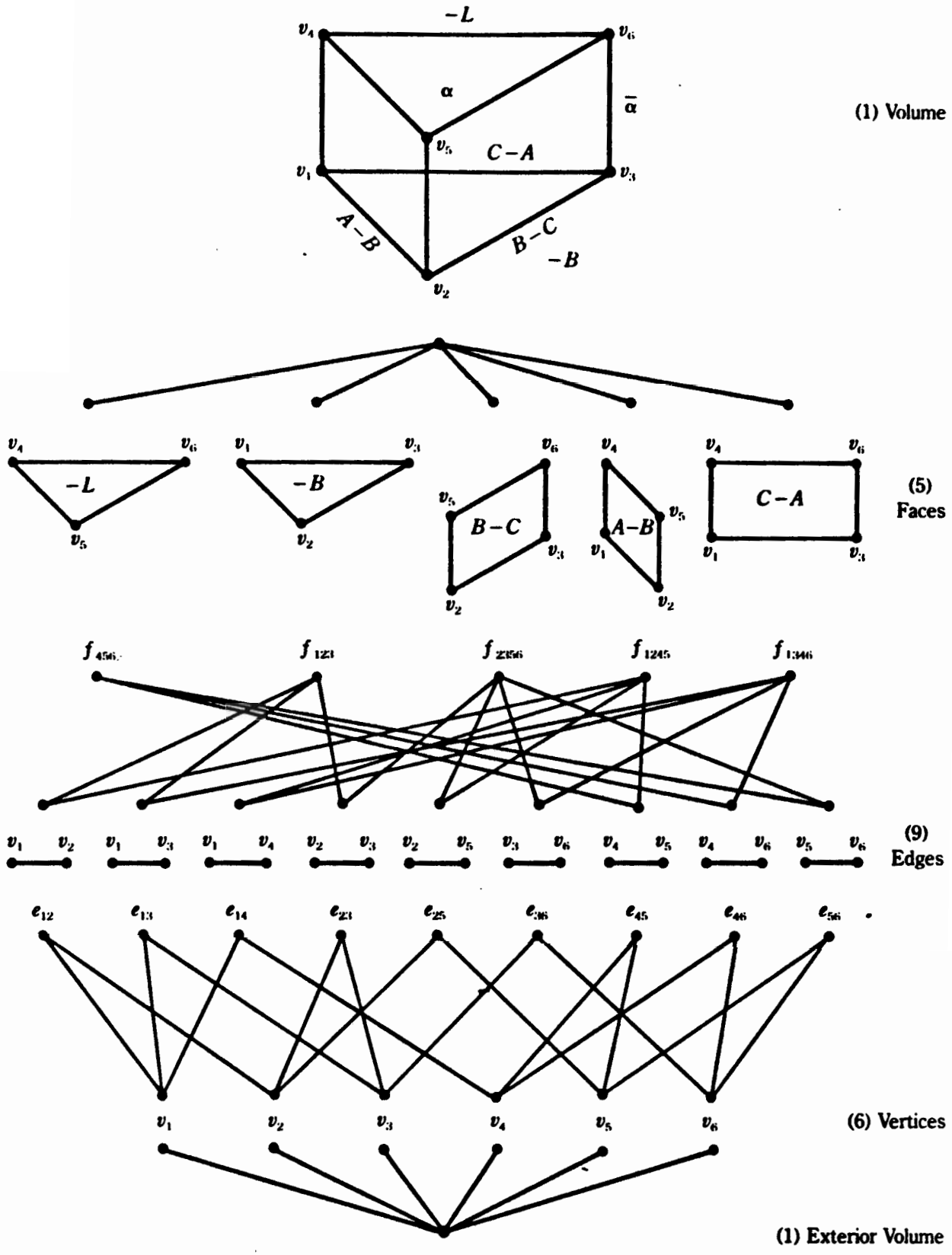

Figure 2. The topological decomposition of the ternary coordinate shell P [A, B, C], or "prism". The connectivity of the vertices, edges and faces are modeled by the incidence sets of table I, and is isomorphic to the graphically depicted lattice of figure 3.

corresponding to e_{12} is {A-B,-B,α}. A face (*2-face*) separates two volumes, and hence the incidence set corresponding to a face will always contain the two labels of the volumes to either side. (The same is true of edges in a binary diagram, and in general for the *(n-1)-faces* of a n-ary diagram.)

INCIDENCE LATTICE FOR P[A,B,C]			
Name	Incidence Set (*Name**)	Interpretation as *k-face*	Maximal Vertex Set
$\bar{\alpha}$	{A-B,B-C,C-A,-B,-L,α}	exterior of P[A,B,C] (volume)	{}
v_1	{C-A,A-B,-B,α}	vertex v_1	$\{v_1\}$
v_2	{A-B,B-C,-B,α}	vertex v_2	$\{v_2\}$
v_3	{B-C,C-A,-B,α}	vertex v_3	$\{v_3\}$
v_4	{C-A,A-B,-L,α}	vertex v_4	$\{v_4\}$
v_5	{A-B,B-C,-L,α}	vertex v_5	$\{v_5\}$
v_6	{B-C,C-A,-L,α}	vertex v_6	$\{v_6\}$
e_{12}	{A-B,-B,α}	edge connecting v_1 and v_2	$\{v_1,v_2\}$
e_{13}	{C-A,-B,α}	edge connecting v_1 and v_3	$\{v_1,v_3\}$
e_{14}	{A-B,C-A,α}	edge connecting v_1 and v_4	$\{v_1,v_4\}$
e_{23}	{B-C,-B,α}	edge connecting v_2 and v_3	$\{v_2,v_3\}$
e_{25}	{A-B,B-C,α}	edge connecting v_2 and v_5	$\{v_2,v_5\}$
e_{36}	{B-C,C-A,α}	edge connecting v_3 and v_6	$\{v_3,v_6\}$
e_{45}	{A-B,-L,α}	edge connecting v_4 and v_5	$\{v_4,v_5\}$
e_{46}	{C-A,-L,α}	edge connecting v_4 and v_6	$\{v_4,v_6\}$
e_{56}	{B-C,-L,α}	edge connecting v_5 and v_6	$\{v_5,v_6\}$
f_{123}	{-B,α}	face at bottom	$\{v_1,v_2,v_3\}$
f_{456}	{-L,α}	face at top	$\{v_4,v_5,v_6\}$
f_{1245}	{A-B,α}	binary system A-B	$\{v_1,v_2,v_4,v_5\}$
f_{1346}	{C-A,α}	binary system C-A	$\{v_1,v_3,v_4,v_6\}$
f_{2356}	{B-C,α}	binary system B-C	$\{v_2,v_3,v_5,v_6\}$
α	{α}	interior volume	$\{v_1,\cdots,v_6\}$

TABLE I

The entire collection of 22 incidence sets constituting the lattice for P[A,B,C] will be denoted by $T_{P[A,B,C]}$. This set $T_{P[A,B,C]}$ implicitly contains all the topological information about P[A,B,C]. Furthermore, there are simple operations on the incidence sets which allow one to determine if the substructure relation holds and to compute the join and meet operations for a given *i-face* and *j-face*, i.e., calculate the answers to questions of type (1)-(4).

We will use the notation "*name**" to refer to the incidence set associated with "name", e.g., f^*_{123} = {-B,α}.

The substructure relation $<$ is calculated by

$$i\text{-}face < j\text{-}face \text{ if and only if } i\text{-}face^* \supset j\text{-}face^*$$

That is, *i-face* is a substructure of *j-face* if and only if *j-face** is a subset of *i-face**. Hence to answer questions of type (1), the determination of the substructures of a given *i-face*, we find all incidence sets of $T_{P[A,B,C]}$ which contain the incidence set *i-face** as a subset.

For example, the edges and vertices of face f_{123}, are found by finding all the sets s (except $\bar{\alpha}$, whose role will become clear in a moment) of $T_{P[A,B,C]}$ such that f^*_{123} is a subset of s. These sets are $e^*_{12}, e^*_{13}, e^*_{23}, v^*_1, v^*_2, v^*_3$, and are the incidence sets for the *k-faces* of lower dimensionality contained within f_{123}. The edges contained in this set are easily identifiable, e.g., in this example all edges have three elements in their corresponding e_i^*. Note that only elements of dimensionality lower than that of f_{123} need be searched. A similar process answers questions of type (2) except we must search for subsets instead of supersets.

In general, questions of type (1) and (2) may be rephrased as:

(1) For a given *k-face*, which *j-faces*, $j < k$, does it contain?

(2) For a given *k-face*, which *j-faces*, $j > k$, contain it?

We call (1) and (2) the substructure and suprastructure question, and use the notation

$$SUB(k\text{-}face^*) \equiv \{j\text{-}face^* \in T_{P|A,B,C]} | j\text{-}face^* \supset k\text{-}face^*\}$$

$$SUP(k\text{-}face^*) \equiv \{j\text{-}face^* \in T_{P|A,B,C]} | j\text{-}face^* \subset k\text{-}face^*\}$$

to denote the set of *j-faces* strictly contained in and containing the given *k-face*. They are both easily answered by searching the lattice elements for the sets containing or contained in the incidence set for the given *k-face*.

Questions of type (3) and (4) utilize two given elements and hence may be regarded as binary operators on $T_{P|A,B,C]}$. Type (3) questions correspond to the join operator and are calculated by

$$i\text{-}face \uparrow j\text{-}face = k\text{-}face \text{ if and only if } k\text{-}face^* = i\text{-}face^* \cap j\text{-}face^*$$

That is, the incidence set of the element corresponding to the join is found by taking the intersection (the set containing elements common to both) of the two incidence sets corresponding to the given *i-face* and *j-face*.

For example, to find out which face of lowest dimensionality contains both the edges e_{12} and e_{13}, we compute the intersection of e_{12}^* and e_{13}^* and obtain f_{123}^*, the common face. For edges e_{12} and e_{36}, their intersection is $\{\alpha\}=\alpha^*$, the volume containing both, since they do not have a common face. Type (3) questions may be generalized to:

(3) Given an *i-face* and a *j-face*, which *k-face*, $k \geq max(i,j)$, of lowest dimensionality, contains them both?

We denote this question and the resulting value by:

$$JOIN(i\text{-}face^*, j\text{-}face^*) \equiv i\text{-}face^* \cap j\text{-}face^*$$

The solution to type (4) questions is more complex. It is calculated by:

$$\begin{aligned} i\text{-}face \downarrow j\text{-}face = k\text{-}face \text{ if and only if } k\text{-}face^* &= \bigcap\{s \in T_{P|A,B,C]} | s \supset i\text{-}face^* \text{ and } s \supset j\text{-}face^*\} \\ &= \bigcap\{s \in T_{P|A,B,C]} | s \in SUB(i\text{-}face^*) \cap SUB(j\text{-}face^*)\} \\ &= JOIN(s_1, \cdots, s_m),\ s_i \in SUB(i\text{-}face^*) \cap SUB(j\text{-}face^*) \end{aligned}$$

In words, we must find the substructure incidence sets common to both the given *i-face** and *j-face**, (a set of sets), and then calculate the set of elements common to all these sets. The resulting set is the incidence set corresponding to the desired *k-face*. Note that this is equivalent to finding the JOIN of all the substructures common to *i-face* and *j-face*.

For example, to find the element of highest dimensionality common to both f_{1245}^* and f_{456}^*, we first find all supersets containing both f_{1245}^* and f_{456}^*. Note that this is equivalent to finding the intersection of SUB(f_{1245}) and SUB(f_{456}). The result is $\{\bar{\alpha}^*, e_{45}^*\}$. We next take the intersection(which is equivalent to JOIN($\bar{\alpha}^*, e_{45}^*$), of these sets which yields e_{45}^*, i.e., edge e_{45} which is common to both. As a further example, we calculate the edge common to f_{123} and f_{456}. The first step yields $\{\bar{\alpha}^*\}$, and since the intersection of a singleton is that singleton, the second step yields $\bar{\alpha}^*$. The interpretation of this result is that there is no *k-face* (edge or vertex) shared by f_{123} and f_{456}. The role of the incidence set $\bar{\alpha}^*$ is to deny the existence of tentatively hypothesized *k-faces*.

Type (4) questions may be generalized to:

(4) Given an *i-face* and a *j-face*, which *k-face*, $k \leq min(i,j)$, of highest dimensionality is contained in both? (If it does not exist, so indicate).

We denote this question and the resulting value by:

$$MEET(i\text{-}face^*, j\text{-}face^*) \equiv JOIN(s_1, \cdots, s_m),\ s_i \in SUB(i\text{-}face^*) \cap SUB(j\text{-}face^*)$$

By combining the two relations SUB and SUP and the binary operators JOIN and MEET to create expressions, complex questions concerning the topological relationships among the equilibria may be

easily stated and efficiently answered by the corresponding incidence sets. For example, a (binary) eutectic is searched for by finding phases α, β, and L and incidence sets L^*, $(\alpha+L)^*$, $(\beta+L)^*$ and $(\alpha+\beta)^*$, such that their joint meet is a *0-face*, i.e., the eutectic.

Questions of type (5) relate to sub-lattices of $T_{P[A,B,C]}$, namely one for each of the binary system faces: $T_{A\text{-}B}$, $T_{B\text{-}C}$ and $T_{C\text{-}A}$, and are easily found, since the incidence sets for each contain the binary system tag, e.g., A-B. The set $T_{P[A,B,C]}$ may be built from $T_{A\text{-}B}$, $T_{B\text{-}C}$ and $T_{C\text{-}A}$ and knowledge of additional 3-dimensional *k-faces*. This will not be developed at this point other than to indicate that the relationships between the constituant (n-1)-ary subsystems and the resulting n-ary system are naturally reflected in the lattice corresponding to the n-ary system.

5. WHERE DID THE LATTICE ELEMENTS $T_{P[A,B,C]}$ COME FROM?

The mathematical relationships existing between the *f-equilibria*, as we have described them in the preceding sections, are a special type of mathematical lattice[6], or in the case of a n-dimensional polytope complex for which n-ary phase diagrams are an example, a polytope face (incidence) lattice[9].

Up to this point we have used the term incidence lattice to refer ambiguously to both the abstract mathematical relationships existing between the topological elements (i.e., *k-faces* denoting the *f-equilibria* of a phase diagram), and the collection of incidence sets which "implement" it. In [9], reference is made to the former. To our knowledge, the existence of the incidence sets modeling the incidence lattice has not been previously known. Therefore, we make the following distinction. For a given phase diagram P, the collection of incidence sets modeling the abstract incidence lattice, we shall refer to as the incidence calculus , and denote this latter by T_P.

Hence, the abstract mathematical relations denoted by the substructure relation $<$, join $\uparrow$ and meet $\downarrow$ are properly part of the incidence lattice, while the operations of SUB, SUP, JOIN and MEET are part of the incidence calculus, and operate on incidence sets. The incidence calculus, $T_{P[A,B,C]}$, because it models a mathematical lattice, has the properties of a lattice, and hence can be depicted in the form of a directed graph[6], called a Hasse diagram, as in figure 3. Note that its structure is identical to the substructure relations exhibited by figure 2.

A remarkable mathematical fact is that the incidence lattice is an atomic lattice and as a result, the v_i's are generators for all the remaining elements of the incidence calculus. We have discovered a practical algorithm for accomplishing this which we have implemented, and have used it to compute the calculus associated with a number of binary, ternary and quaternary phase diagram topologies.

Assume we have been given a set of vertex incidence sets v_i^*, $i=1,2,\cdots,v$. The algorithm may best be understood by first thinking about a naive version which enumerates all combinations of $\{v_1^*, v_2^*, \ldots, v_v^*\}$, from v at a time down to 0 at a time. The intersection of each combination is found, and for a particular intersection value, that value and the largest set of v_i^*'s giving that value are the incidence set and maximal vertex set respectively, associated with a unique element of the topological decomposition. For the prism of figure 2, whose incidence calculus is given in table I, column four lists the corresponding maximal vertex set. In effect, we are generating the closure under intersection for the given set of v_i^*'s. The algorithm is based on the following recursive definition in which the set of combinations are defined in terms of lower order combinations.

Let $[v_1, v_2, \cdots, v_v \mid i]$ denote the set of combinations of v vertices taken i at a time, and let $*$ be the operation of distributive union defined on a singleton $\{v\}$ and a set of sets S_i by:

$$\{v\} * \{S_1, S_2, \cdots, S_k\} \equiv \{\{v\} \cup S_1, \{v\} \cup S_2, \cdots, \{v\} \cup S_k\}$$

Then the set of v vertices taken i at a time may be recursively computed by the following[10]:

$$[v_1, v_2, \cdots, v_v \mid i] = \begin{cases} \{v_v\} * [v_1, v_2, \cdots, v_{v-1} \mid i-1] \cup \{v_{v-1}\} * [v_1, v_2, \cdots, v_{v-2} \mid i-1] \cup \cdots \\ \qquad \cdots \cup \{v_v\} * [v_1, v_2, \cdots, v_{i-1} \mid i-1] & 1 < i \leq v \\ \{\{v_1\}, \{v_2\}, \cdots, \{v_v\}\} & i = 1 \\ \{\} & i = 0 \end{cases}$$

This is depicted in figure 4 for the ternary prism of figure 2, where the v_i^*'s in all combinations are listed with $[v_1, v_2, \cdots, v_6 \mid 6]$ at the top, $[v_1, v_2, \cdots, v_6 \mid 5]$ below, down to $[v_1, v_2, \cdots, v_6 \mid 0]$ at the bottom. Combinations of vertices resulting in maximal intersection values are marked with asterisks.

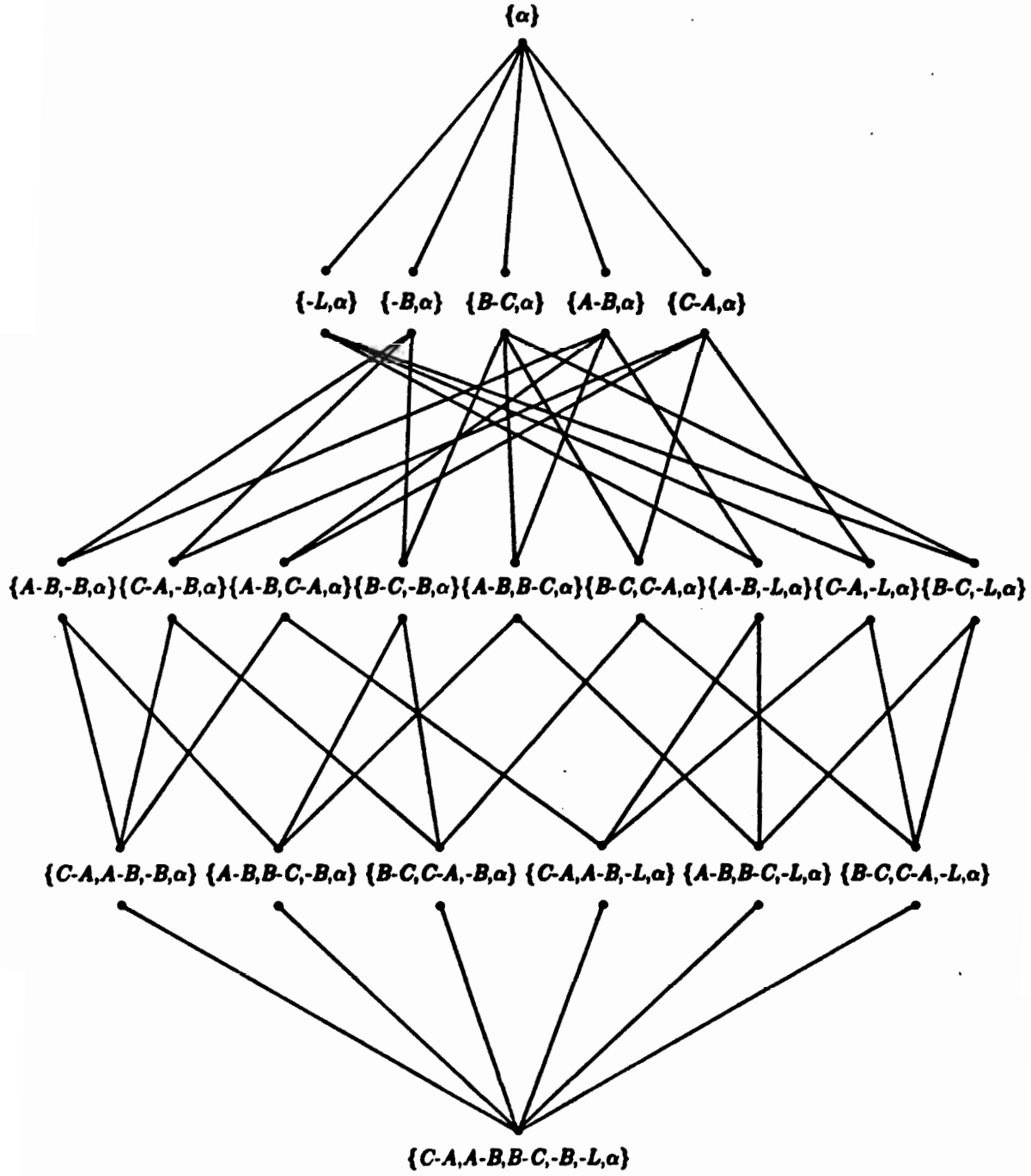

Figure 3. The 22 incidence sets corresponding to the interior volume (at top of figure), 5 faces, 9 edges, 6 vertices and exterior volume (bottom), for the ternary prism of figure 2, in which the substructure, suprastructure, meet and join are modeled by the lines connecting them.

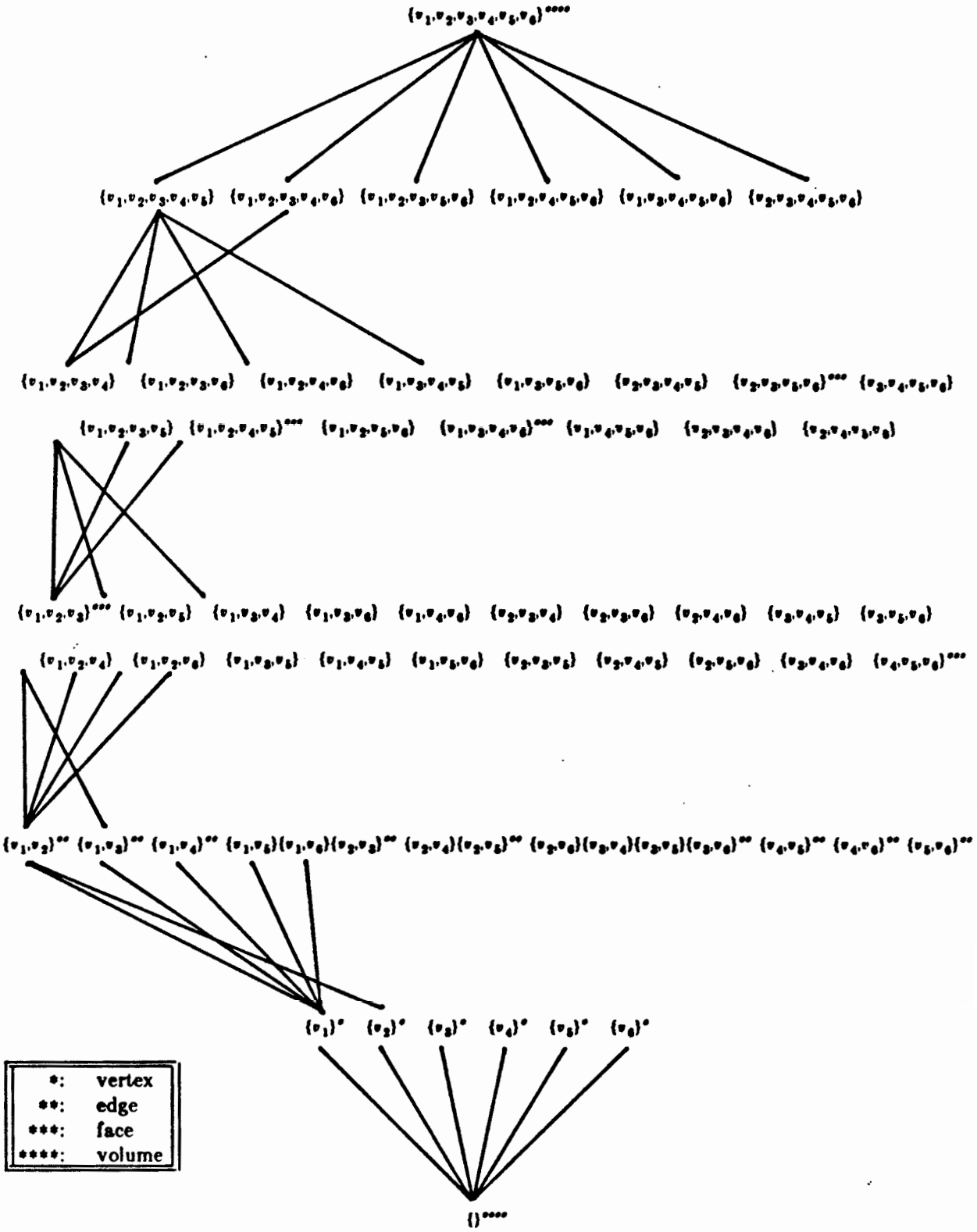

Figure 4. The Hasse diagram for the 64 combinations of six vertices taken i at a time listed by decreasing i from 6 to 0 from top to bottom. The intersections of the 22 elements with asterisks correspond to the incidence sets for the 6 vertices, 9 edges, 5 faces and interior and exterior volumes for the ternary prism of figure 2. (Lines, indicating the subset relation, have been drawn for just the left-most combinations, in order to simplify the figure.)

Finding all maximal vertex sets in this manner will require that $\sum_{i=0}^{v}\binom{v}{i} = 2^v$ combinations† be tested and hence it will be computationally too expensive to compute the incidence sets for a very complex phase diagram. However, the above computation may be modified slightly so as to reduce the average computational complexity from being exponential in v to polynomial in v. This modification and subsequent reduction in computation stems from two observations: (a) If the intersection of a combination is empty, then all combinations which contain that combination as a subset will also be empty and need not be generated, and (b), any subcombination contained in a (known) maximal combination whose value is the same as the maximal one need not be generated. (a) in fact, is a special case of (b).

The v_i^*'s are initially obtained by applying the following steps to a n-ary phase diagram:

(1) Uniquely label the *0-faces* (vertices) and highest dimensional *n-faces* (volumes for $n=3$).

(2) For each v_i, v_i^* is the set of *n-face* labels incident on v_i.

Step 1 above requires labeling the exterior volume in a manner which uniquely characterizes each face. This is easily performed. As a check to insure that the given v_i^* describe a topologically consistant figure, the generalized Euler identity, i.e., Schlaefli identity[4,8] may be applied to the resulting *i-faces*'. Let *#(i-face)* denote the number of distinct *i-faces* of dimension i, in a n-dimensional n-ary phase diagram. Then this identity requires that

$$\sum_{i=0}^{n} \#(i\text{-face})(-1)^i = 1+(-1)^n$$

and reduces to the respective 2 and 3 dimensional Euler identities *vertices -edges +faces*=2 and *vertices -edges +faces-volumes* =0, for $n=2$ and 3.

A mathematical lattice[6] must contain two special elements, the greatest lower bound(GLB) and the least upper bound(LUB). These two elements are such that for all elements x in the lattice, $GLB < x$ and $x < LUB$, i.e., they are respectively a suprastructure and substructure of every other element, and hence $GLB \downarrow x = GLB$ and $LUB \uparrow x = LUB$. In the case of $T_{P[A,B,C]}$, $\bar{\alpha}^*$ served as the GLB and α^* as the LUB. In general, and more to the point, real phase diagrams will contain interior *k-faces* or *f-equilibria*, so that we may think of a n-ary phase diagram as a complex of *n-equilibria*. In this case, the LUB must correspond, not to a single *n-equilibria* as in $T_{P[A,B,C]}$, but to the entire assembly or complex of *f-equilibria*. It turns out that within the incidence calculus, the empty set {} models the desired behavior of the LUB of the lattice. Hence if the join of two elements maps to the empty set, the interpretation is that they have only the full diagram complex in common. Note that the LUB is not a true *i-face* and is not to be counted in the Schlaefli identity.

The incidence calculus GLB is in general analogous to the incidence set for $\bar{\alpha}$ of $T_{P[A,B,C]}$: It consists of all labels assigned to the interior *n-equilibria* (*n-faces*) plus the labels assigned to the $n+2$ regions the exterior of the diagram must be divided into. The $n+2$ regions and their respective labels correspond to the n subsytem faces and the upper and lower temperature truncations.

In figure 5 we depict the binary eutectic system cadmium-zinc[11] with the vertices labeled v_i, $i=1,2,\cdots,11$. The interior *2-equilibria* (phase fields) have been labeled, but in addition, the region exterior to the border has been broken up into four regions by diagonal lines extending out from the four corners of the diagram. It is convienent at this point to think of the phase diagram as being drawn on the front of a balloon, so that the extension of these diagonals meet at a vertex at the back of the balloon, and hence divide the region exterior to the phase diagram into four regions, or *2-faces*, covering the back of the balloon. These four regions correspond to the border resulting from the two unary subsystems and the two temperature truncations, and hence are labeled *-Cd*,*-Zn* and *-Top*,*-Base* respectively. The incorporation of "-" in a label, while not needed by the algorithm, indicates that these are exterior labels, in the same way that r "+" signs in a phase field label indicate that there are $r+1$ phases present.

Although we have not done so, the twelfth vertex at the rear of the balloon, whose incidence set is {*-Cd*,*-Zn*,*-Top*,*-base*}, could be added to the other eleven so that the incidence calculus would account for the entire surface of the balloon, including the exterior faces and their mutual borders.

† We use the notation $\binom{v}{i}$ to denote the number of combinations of v things taken i at a time, whose value is given by $\frac{v!}{i!(v-i)!}$.

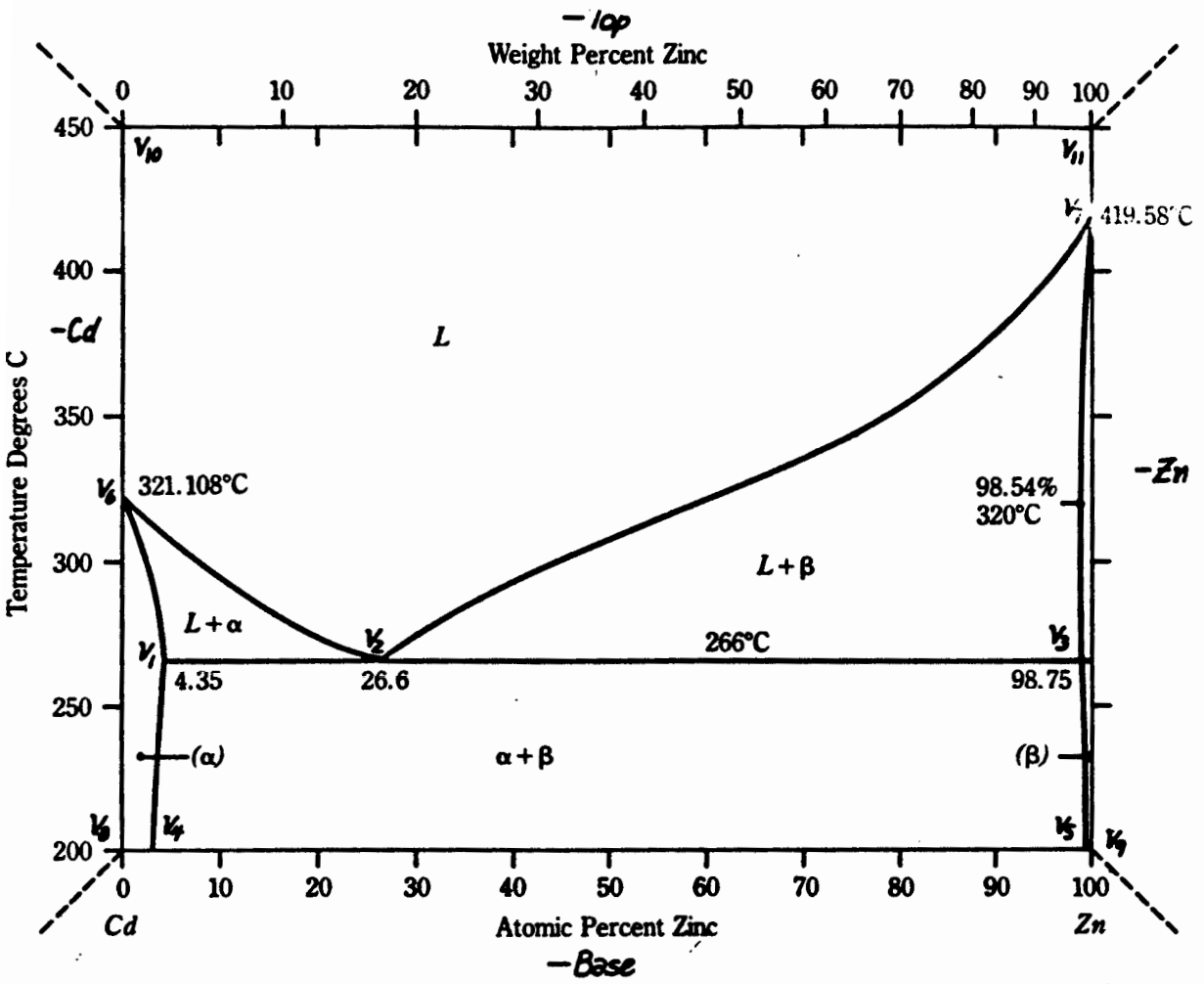

Figure 5. The eutectic system cadmium-zinc taken from [11], with the vertices annotated by v_i, $i = 1, 2, \ldots, 11$. The connectivity of the phase equilibria are modeled by the incidence calculus of table II.

Cadmium-Zinc Equilibria Incidence Calculus							
K	Index	Vertex Set	Incidence Set	K	Index	Vertex Set	Incidence Set
Vertices	1	$\{v_1\}$	$\{\alpha, L+\alpha, \alpha+\beta\}$	Edges	1	$\{v_1, v_2\}$	$\{L+\alpha, \alpha+\beta\}$
	2	$\{v_2\}$	$\{L+\alpha, L, L+\beta, \alpha+\beta\}$		2	$\{v_1, v_4\}$	$\{\alpha, \alpha+\beta\}$
	3	$\{v_3\}$	$\{\beta, L+\beta, \alpha+\beta\}$		3	$\{v_1, v_6\}$	$\{\alpha, L+\alpha\}$
	4	$\{v_4\}$	$\{\alpha, \alpha+\beta, \text{-}Base\}$		4	$\{v_2, v_3\}$	$\{L+\beta, \alpha+\beta\}$
	5	$\{v_5\}$	$\{\beta, \alpha+\beta, \text{-}Base\}$		5	$\{v_2, v_6\}$	$\{L+\alpha, L\}$
	6	$\{v_6\}$	$\{\alpha, L+\alpha, L, \text{-}Cd\}$		6	$\{v_2, v_7\}$	$\{L, L+\beta\}$
	7	$\{v_7\}$	$\{\beta, L+\beta, L, \text{-}Zn\}$		7	$\{v_3, v_5\}$	$\{\beta, \alpha+\beta\}$
	8	$\{v_8\}$	$\{\alpha, \text{-}Cd, \text{-}Base\}$		8	$\{v_3, v_7\}$	$\{\beta, L+\beta\}$
	9	$\{v_9\}$	$\{\beta, \text{-}Zn, \text{-}Base\}$		9	$\{v_4, v_5\}$	$\{\alpha+\beta, \text{-}Base\}$
	10	$\{v_{10}\}$	$\{L, \text{-}Cd, \text{-}Top\}$		10	$\{v_4, v_8\}$	$\{\alpha, \text{-}Base\}$
	11	$\{v_{11}\}$	$\{L, \text{-}Zn, \text{-}Top\}$		11	$\{v_5, v_9\}$	$\{\beta, \text{-}Base\}$
Faces	1	$\{v_1, v_2, v_3, v_4, v_5\}$	$\{\alpha+\beta\}$		12	$\{v_6, v_8\}$	$\{\alpha, \text{-}Cd\}$
	2	$\{v_2, v_6, v_7, v_{10}, v_{11}\}$	$\{L\}$		13	$\{v_6, v_{10}\}$	$\{L, \text{-}Cd\}$
	3	$\{v_1, v_4, v_6, v_8\}$	$\{\alpha\}$		14	$\{v_7, v_9\}$	$\{\beta, \text{-}Zn\}$
	4	$\{v_3, v_5, v_7, v_9\}$	$\{\beta\}$		15	$\{v_7, v_{11}\}$	$\{L, \text{-}Zn\}$
	5	$\{v_1, v_2, v_6\}$	$\{L+\alpha\}$		16	$\{v_{10}, v_{11}\}$	$\{L, \text{-}Top\}$
	6	$\{v_2, v_3, v_7\}$	$\{L+\beta\}$				
LUB	1	$\{v_i\}_{i=1,11}$	$\{\}$	GLB	1	$\{\}$	$\{\alpha+\beta, L+\alpha, L+\beta, \alpha, \beta, \text{-}Base, \text{-}Cd, L, \text{-}Zn, \text{-}Top\}$

TABLE II

Table II lists the incidence sets which model the topology or "incidences" of the P[Cd,Zn] system as depicted in figure 5. (Without the twelfth vertex.) The incidence sets corresponding to the 11 vertices($k=0$), 16 edges($k=1$) and 7 faces($k=2$) are enumerated, as well as the maximal set of vertices(Vertex Set) whose intersection yields that incidence set. The GLB and LUB are given, but note that only the GLB must be counted as a *2-face*, in the identity 11-16+7=2.

The incidence set v_i^* corresponding to the v_i may be read directly off figure 5. For example, v_1 is located at the junction of phase fields α, $L+\alpha$ and $\alpha+\beta$ and hence all three are incident on v_1 so that $v_1^*=\{\alpha, L+\alpha, \alpha+\beta\}$. Once these v_i^*'s have been determined, the remaining faces and edges may be algorithmically generated from them.

In the fourth column of table I we have listed for each incidence set, the (unique) maximal set of vertices whose intersection yields that incidence set (as described above). But in fact, these vertex sets are a second "dual" incidence calculus which models the inverted mathematical lattice, or dual space[4,8], in which the role of vertices and faces is interchanged. For example, the topological dual for the prism of figure 2 is obtained by mapping the 6 vertices, 9 edges and 5 faces to a polyhedra containing 6 faces, 9 edges and 5 vertices, respectively, while simultaneosly reversing the sense of the substructure $<$ relation. The resulting polyhedra is a "double pyramid", obtained from a triangular base, with an "apex" vertex to either side of this face joined to each of the vertices of the base. The incidence calculus for this dual has the same structure as that of figure 3, but inverted, i. e., figure 3 turned upside down so that what were the vertices at the bottom, become the faces at the top, and the incidence sets replaced by their respective maximal vertex sets.

The operation of taking the dual is well defined for polytope "shells", such as the prism, but since a phase diagram contains structure internal to its border, or shell, its topological dual is more easily visualized by thinking of it again as being drawn on the surface of a (n+1)-dimensional sphere, where it may be subsequently thought of as a (n+1)-dimensional polytope in which the phase fields become the facets of the polytope. For example, the topological dual for a binary ($n=2$) phase diagram is obtained by treating it as graph drawn on a sphere where its graph dual[19] is generated. This dual is obtained by treating the phase field labels as the new vertices (graph nodes), and then connecting those vertices by edges whose corresponding phase fields were adjoining one another in the original diagram. More generally, in an n-ary phase diagram, the geometric role of the *(n-k)-faces* and the *k-faces*, $k=0,1,\cdots,n$, are interchanged in the dual, while simultaneously interchanging the substructure/suprastructure relation. More precisely, let $\overline{k\text{-face}}$ denote the *(n-k)-face* dual of *k-face*. Then for a maximal vertex set $v_{i_1}, v_{i_2}, \cdots, v_{i_m}$, $k=0,1,2,\cdots,n$,

$$k\text{-face}^* = v_{i_1}^* \cap v_{i_2}^* \cap \cdots \cap v_{i_m}^* \quad \text{if and only if} \quad \overline{k\text{-face}}^* = \{v_{i_1}, v_{i_2}, \cdots, v_{i_m}\}$$

Hence, the algorithm we have described for computing the incidence calculus for a given phase diagram automatically generates the incidence calculus for its dual, in the form of the set of its maximal vertex sets. This duality relationship can be exploited in the following way. In a n-ary system, the *k-faces* and the *(n-k)-faces* are duals and this is reflected in the fact that their corresponding incidence sets are "inversions" of each other. For $k=0$ for example, we can invert the vertices, mapping them into the incidence sets for the dual *n-faces*, by the following procedure: For each *n-face* label L, we list the set of vertices v_i for which the label L is a member of v_i's incidence set. This results in the maximal *n-face* set for L or dual incidence set for "vertex" $\overline{L}$.

For example, in table II, L appears in the incidence sets for vertices v_2, v_6, v_7, v_{10}, and v_{11}, and hence the dual incidence set for L is $\overline{L}^*=\{v_2, v_6, v_7, v_{10}, v_{11}\}$, which is the maximal set of vertices whose intersection is $\{L\}$.

The practical consequences of all of this is that once the v_i^*'s have been determined, the remaining incidence sets can be generated from either the v_i^*'s or from the dual incidence sets for the *n-faces*. In table II, for example, we can generate the incidence calculus by taking combinations of the face vertex sets. Since there are much fewer combinations in 6 faces than in 11 vertices, the computation required will be much less, and in general, since the number of phase fields is much fewer than the number of vertices, it will be less expensive computationally to generate the incidence calculus from the *n-faces*. But the *n-faces* can be generated from the v_i^*'s by inverting them, so in fact we can start with either the vertex incidence sets or the *n-face* incidence sets. This combined with the method we have discovered for reducing the number of combinations which must be searched is the basis for a practical algorithm for generating the incidence calculus for phase diagrams.

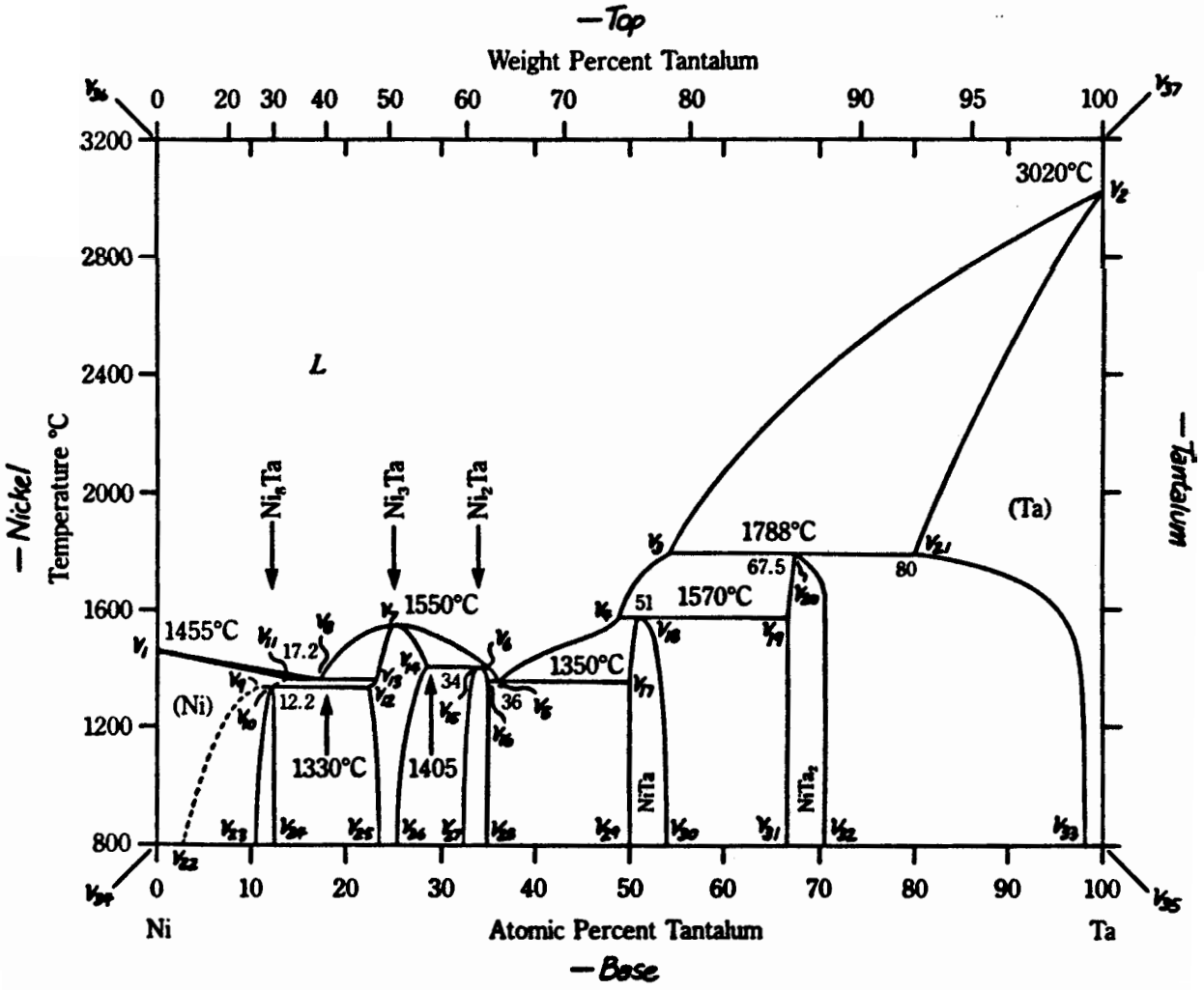

Figure 6. The nickel-tantalum system taken from [12]. The vertices are annotated by v_i, $i = 1, 2, \ldots, 37$, and provide the vertex incidence sets from which the remaining topological relationships may be calculated. Its incidence calculus is given in table III.

A more complex binary, the nickel-tantalum system, taken from [12], and with the vertices labeled v_i, $i=1,2\cdots,37$ is graphically depicted in figure 6. The incidence calculus is given in table III, and in fact, since the number of phase fields is 26 and the number of vertices is 37, was calculated by inverting the vertices, calculating the dual, and listing the dual maximal vertex sets as the originally desired incidence sets.

In order for distinct *i-faces* to map to distinct *i-face'* incidence sets, the incidence calculus requires that the *i-faces* be incident upon distinct sets of vertices This is not strictly true for all *f-equilibria*. For example, in a binary isomorphous system, i. e., complete solubility at all compositions as in the binary subsystem A-B in the ternary of figure 8, the solidus and liquidus boundaries as well as the $L+\alpha$ phase field are all incident on the same vertices, namely $v_1^* = \{-Component_1, \alpha, L+\alpha, L\}$ and $v_2^* = \{-Component_2, \alpha, L+\alpha, L\}$. As a result, their join, $v_1 \uparrow v_2$ is not unique, but consists of both the solidus and liquidus boundaries. The incidence calculus reflects this by producing for $v_1 \uparrow v_2$, $v_1^* \cap v_2^* = \{\alpha, L+\alpha, L\}$, which is correct topologically but unexpected. That it is correct topologically may be seen by interchanging the solidus and liquidus boundaries, i. e., changing just metric attributes, and noting that v_1^* and v_2^* remain the same. This incidence set must be interpreted as modeling all three, namely, the solidus and liquidus boundaries and the $L+\alpha$ phase field separating them, since the intersection of the two (identical) boundary incidence sets is again the same boundary incidence set. In table V, containing the incidence calculus for the ternary of figure 8, this has happened to edge 31. In general, this will happen in a n-ary phase diagram when two $(n-1)$-*faces* are incident on the same vertices, i.e., are "parallel".

When this happens, it may be detected algorithmically, by applying an identity relating the number of vertices v in the associated intersection, the number of elements p in the resulting intersection value and the dimension n, i.e., if $v=n$, then $v+p = n+2$. For example, in a binary system($n=2$), an edge is incident on two vertices($v=2$), and separates two phase fields($p=2$), and hence $2+2 = 2+2$. For the incidence set $\{\alpha, L+\alpha, L\}$ this does not hold since $p=3$.

For ternary diagrams, two incidence sets may have to be mutually interpreted. For example, the three phase region $L+\alpha+\beta$ of figure 8 and two of this regions faces have mutually identical incidences. The algorithm we have described generates the incidence sets $\{L+\alpha, \alpha+\beta, L+\alpha+\beta\}$ and $\{L+\beta, \alpha+\beta, L+\alpha+\beta\}$, but these must be interpreted as the volume $\{L+\alpha+\beta\}$, and the two faces $\{L+\alpha, L+\alpha+\beta\}$ and $\{L+\beta, L+\alpha+\beta\}$. We have not worked all the rules, but believe that all such cases are amenable to algorithmic interpretation.

The problem of non-unique incidence sets may also be solved by introducing "pseudo" vertices. For example, the melting point vertex of an isomorphous system may be replaced by two vertices, both at the same metric coordinates, but incident on distinct sets of phase fields.

TABLE III: Nickel-Tantalum Incidence Calculus

K	Index	Vertex Set	Incidence Set
Vertices	1	$\{v_8\}$	$\{Ni+L, Ni+Ni_3Ta, L+Ni_3Ta, L\}$
	2	$\{v_1\}$	$\{Ni+L, Ni, -Nickel, L\}$
	3	$\{v_{10}\}$	$\{Ni+Ni_3Ta, Ni+Ni_8Ta, Ni_8Ta, Ni_8Ta+Ni_3Ta\}$
	4	$\{v_7\}$	$\{L+Ni_3Ta, Ni_3Ta+L, Ni_3Ta, L\}$
	5	$\{v_{15}\}$	$\{Ni_3Ta+L, Ni_2Ta+L, Ni_3Ta+Ni_2Ta, Ni_2Ta\}$
	6	$\{v_5\}$	$\{Ni_2Ta+L, L+NiTa, Ni_2Ta+NiTa, L\}$
	7	$\{v_{18}\}$	$\{L+NiTa, L+NiTa_2, NiTa, NiTa+NiTa_2\}$
	8	$\{v_{20}\}$	$\{L+NiTa_2, L+Ta, NiTa_2, NiTa_2+Ta\}$
	9	$\{v_2\}$	$\{L+Ta, Ta, -Tantalum, L\}$
	10	$\{v_{11}\}$	$\{Ni+L, Ni+Ni_3Ta, Ni\}$
	11	$\{v_{13}\}$	$\{Ni+Ni_3Ta, L+Ni_3Ta, Ni_3Ta\}$
	12	$\{v_9\}$	$\{Ni+Ni_3Ta, Ni+Ni_8Ta, Ni\}$
	13	$\{v_{12}\}$	$\{Ni+Ni_3Ta, Ni_8Ta+Ni_3Ta, Ni_3Ta\}$
	14	$\{v_6\}$	$\{Ni_3Ta+L, Ni_2Ta+L, L\}$
	15	$\{v_{14}\}$	$\{Ni_3Ta+L, Ni_3Ta, Ni_3Ta+Ni_2Ta\}$
	16	$\{v_{16}\}$	$\{Ni_2Ta+L, Ni_2Ta, Ni_2Ta+NiTa\}$
	17	$\{v_4\}$	$\{L+NiTa, L+NiTa_2, L\}$
	18	$\{v_{17}\}$	$\{L+NiTa, Ni_2Ta+NiTa, NiTa\}$
	19	$\{v_3\}$	$\{L+NiTa_2, L+Ta, L\}$

TABLE III: Nickel-Tantalum Incidence Calculus

K	Index	Vertex Set	Incidence Set
Vertices	20	$\{v_{19}\}$	$\{L+NiTa_2, NiTa+NiTa_2, NiTa_2\}$
	21	$\{v_{21}\}$	$\{L+Ta, NiTa_2+Ta, Ta\}$
	22	$\{v_{23}\}$	$\{Ni+Ni_8Ta, Ni_8Ta, \text{-}Base\}$
	23	$\{v_{22}\}$	$\{Ni+Ni_8Ta, Ni, \text{-}Base\}$
	24	$\{v_{24}\}$	$\{Ni_8Ta, Ni_8Ta+Ni_3Ta, \text{-}Base\}$
	25	$\{v_{25}\}$	$\{Ni_8Ta+Ni_3Ta, Ni_3Ta, \text{-}Base\}$
	26	$\{v_{26}\}$	$\{Ni_3Ta, Ni_3Ta+Ni_2Ta, \text{-}Base\}$
	27	$\{v_{27}\}$	$\{Ni_3Ta+Ni_2Ta, Ni_2Ta, \text{-}Base\}$
	28	$\{v_{28}\}$	$\{Ni_2Ta, Ni_2Ta+NiTa, \text{-}Base\}$
	29	$\{v_{29}\}$	$\{Ni_2Ta+NiTa, NiTa, \text{-}Base\}$
	30	$\{v_{30}\}$	$\{NiTa, NiTa+NiTa_2, \text{-}Base\}$
	31	$\{v_{31}\}$	$\{NiTa+NiTa_2, NiTa_2, \text{-}Base\}$
	32	$\{v_{32}\}$	$\{NiTa_2, NiTa_2+Ta, \text{-}Base\}$
	33	$\{v_{33}\}$	$\{NiTa_2+Ta, \text{-}Base, Ta\}$
	34	$\{v_{34}\}$	$\{Ni, \text{-}Base, \text{-}Nickel\}$
	35	$\{v_{35}\}$	$\{\text{-}Base, Ta, \text{-}Tantalum\}$
	36	$\{v_{36}\}$	$\{\text{-}Nickel, \text{-}Top, L\}$
	37	$\{v_{37}\}$	$\{\text{-}Tantalum, \text{-}Top, L\}$
Edges	1	$\{v_8, v_{11}\}$	$\{Ni+L, Ni+Ni_3Ta\}$
	2	$\{v_1, v_{11}\}$	$\{Ni+L, Ni\}$
	3	$\{v_1, v_8\}$	$\{Ni+L, L\}$
	4	$\{v_8, v_{13}\}$	$\{Ni+Ni_3Ta, L+Ni_3Ta\}$
	5	$\{v_9, v_{10}\}$	$\{Ni+Ni_3Ta, Ni+Ni_8Ta\}$
	6	$\{v_{10}, v_{12}\}$	$\{Ni+Ni_3Ta, Ni_8Ta+Ni_3Ta\}$
	7	$\{v_{12}, v_{13}\}$	$\{Ni+Ni_3Ta, Ni_3Ta\}$
	8	$\{v_9, v_{11}\}$	$\{Ni+Ni_3Ta, Ni\}$
	9	$\{v_7, v_{13}\}$	$\{L+Ni_3Ta, Ni_3Ta\}$
	10	$\{v_7, v_8\}$	$\{L+Ni_3Ta, L\}$
	11	$\{v_6, v_{15}\}$	$\{Ni_3Ta+L, Ni_2Ta+L\}$
	12	$\{v_7, v_{14}\}$	$\{Ni_3Ta+L, Ni_3Ta\}$
	13	$\{v_{14}, v_{15}\}$	$\{Ni_3Ta+L, Ni_3Ta+Ni_2Ta\}$
	14	$\{v_6, v_7\}$	$\{Ni_3Ta+L, L\}$
	15	$\{v_{15}, v_{16}\}$	$\{Ni_2Ta+L, Ni_2Ta\}$
	16	$\{v_5, v_{16}\}$	$\{Ni_2Ta+L, Ni_2Ta+NiTa\}$
	17	$\{v_5, v_6\}$	$\{Ni_2Ta+L, L\}$
	18	$\{v_4, v_{18}\}$	$\{L+NiTa, L+NiTa_2\}$
	19	$\{v_5, v_{17}\}$	$\{L+NiTa, Ni_2Ta+NiTa\}$
	20	$\{v_{17}, v_{18}\}$	$\{L+NiTa, NiTa\}$
	21	$\{v_4, v_5\}$	$\{L+NiTa, L\}$
	22	$\{v_3, v_{20}\}$	$\{L+NiTa_2, L+Ta\}$
	23	$\{v_{18}, v_{19}\}$	$\{L+NiTa_2, NiTa+NiTa_2\}$
	24	$\{v_{19}, v_{20}\}$	$\{L+NiTa_2, NiTa_2\}$
	25	$\{v_3, v_4\}$	$\{L+NiTa_2, L\}$
	26	$\{v_{20}, v_{21}\}$	$\{L+Ta, NiTa_2+Ta\}$
	27	$\{v_2, v_{21}\}$	$\{L+Ta, Ta\}$
	28	$\{v_2, v_3\}$	$\{L+Ta, L\}$
	29	$\{v_{10}, v_{23}\}$	$\{Ni+Ni_8Ta, Ni_8Ta\}$
	30	$\{v_9, v_{22}\}$	$\{Ni+Ni_8Ta, Ni\}$
	31	$\{v_{22}, v_{23}\}$	$\{Ni+Ni_8Ta, \text{-}Base\}$
	32	$\{v_{10}, v_{24}\}$	$\{Ni_8Ta, Ni_8Ta+Ni_3Ta\}$
	33	$\{v_{23}, v_{24}\}$	$\{Ni_8Ta, \text{-}Base\}$
	34	$\{v_{12}, v_{25}\}$	$\{Ni_8Ta+Ni_3Ta, Ni_3Ta\}$
	35	$\{v_{24}, v_{25}\}$	$\{Ni_8Ta+Ni_3Ta, \text{-}Base\}$
	36	$\{v_{14}, v_{26}\}$	$\{Ni_3Ta, Ni_3Ta+Ni_2Ta\}$
	37	$\{v_{25}, v_{26}\}$	$\{Ni_3Ta, \text{-}Base\}$

TABLE III: Nickel-Tantalum Incidence Calculus

K	Index	Vertex Set	Incidence Set
Edges	38	$\{v_{15}, v_{27}\}$	$\{Ni_3Ta + Ni_2Ta, Ni_2Ta\}$
	39	$\{v_{26}, v_{27}\}$	$\{Ni_3Ta + Ni_2Ta, \text{-}Base\}$
	40	$\{v_{16}, v_{28}\}$	$\{Ni_2Ta, Ni_2Ta + NiTa\}$
	41	$\{v_{27}, v_{28}\}$	$\{Ni_2Ta, \text{-}Base\}$
	42	$\{v_{17}, v_{29}\}$	$\{Ni_2Ta + NiTa, NiTa\}$
	43	$\{v_{28}, v_{29}\}$	$\{Ni_2Ta + NiTa, \text{-}Base\}$
	44	$\{v_{18}, v_{30}\}$	$\{NiTa, NiTa + NiTa_2\}$
	45	$\{v_{29}, v_{30}\}$	$\{NiTa, \text{-}Base\}$
	46	$\{v_{19}, v_{31}\}$	$\{NiTa + NiTa_2, NiTa_2\}$
	47	$\{v_{30}, v_{31}\}$	$\{NiTa + NiTa_2, \text{-}Base\}$
	48	$\{v_{20}, v_{32}\}$	$\{NiTa_2, NiTa_2 + Ta\}$
	49	$\{v_{31}, v_{32}\}$	$\{NiTa_2, \text{-}Base\}$
	50	$\{v_{32}, v_{33}\}$	$\{NiTa_2 + Ta, \text{-}Base\}$
	51	$\{v_{21}, v_{33}\}$	$\{NiTa_2 + Ta, Ta\}$
	52	$\{v_{22}, v_{34}\}$	$\{Ni, \text{-}Base\}$
	53	$\{v_1, v_{34}\}$	$\{Ni, \text{-}Nickel\}$
	54	$\{v_{33}, v_{35}\}$	$\{\text{-}Base, Ta\}$
	55	$\{v_2, v_{35}\}$	$\{Ta, \text{-}Tantalum\}$
	56	$\{v_1, v_{36}\}$	$\{\text{-}Nickel, L\}$
	57	$\{v_2, v_{37}\}$	$\{\text{-}Tantalum, L\}$
	58	$\{v_{36}, v_{37}\}$	$\{\text{-}Top, L\}$
Faces	1	$\{v_1, v_8, v_{11}\}$	$\{Ni + L\}$
	2	$\{v_8, v_9, v_{10}, v_{11}, v_{12}, v_{13}\}$	$\{Ni + Ni_3Ta\}$
	3	$\{v_7, v_8, v_{13}\}$	$\{L + Ni_3Ta\}$
	4	$\{v_6, v_7, v_{14}, v_{15}\}$	$\{Ni_3Ta + L\}$
	5	$\{v_5, v_6, v_{15}, v_{16}\}$	$\{Ni_2Ta + L\}$
	6	$\{v_4, v_5, v_{17}, v_{18}\}$	$\{L + NiTa\}$
	7	$\{v_3, v_4, v_{18}, v_{19}, v_{20}\}$	$\{L + NiTa_2\}$
	8	$\{v_2, v_3, v_{20}, v_{21}\}$	$\{L + Ta\}$
	9	$\{v_9, v_{10}, v_{22}, v_{23}\}$	$\{Ni + Ni_8Ta\}$
	10	$\{v_{10}, v_{23}, v_{24}\}$	$\{Ni_8Ta\}$
	11	$\{v_{10}, v_{12}, v_{24}, v_{25}\}$	$\{Ni_8Ta + Ni_3Ta\}$
	12	$\{v_7, v_{12}, v_{13}, v_{14}, v_{25}, v_{26}\}$	$\{Ni_3Ta\}$
	13	$\{v_{14}, v_{15}, v_{26}, v_{27}\}$	$\{Ni_3Ta + Ni_2Ta\}$
	14	$\{v_{15}, v_{16}, v_{27}, v_{28}\}$	$\{Ni_2Ta\}$
	15	$\{v_5, v_{16}, v_{17}, v_{28}, v_{29}\}$	$\{Ni_2Ta + NiTa\}$
	16	$\{v_{17}, v_{18}, v_{29}, v_{30}\}$	$\{NiTa\}$
	17	$\{v_{18}, v_{19}, v_{30}, v_{31}\}$	$\{NiTa + NiTa_2\}$
	18	$\{v_{19}, v_{20}, v_{31}, v_{32}\}$	$\{NiTa_2\}$
	19	$\{v_{20}, v_{21}, v_{32}, v_{33}\}$	$\{NiTa_2 + Ta\}$
	20	$\{v_1, v_9, v_{11}, v_{22}, v_{34}\}$	$\{Ni\}$
	21	$\{v_2, v_{21}, v_{33}, v_{35}\}$	$\{Ta\}$
	22	$\{v_1, v_2, v_3, v_4, v_5, v_6, v_7, v_8, v_{36}, v_{37}\}$	$\{L\}$
LUB	1	$\{v_i\}_{i=1,37}$	$\{\}$
GLB	1	$\{\}$	$\{Ni + L, Ni + Ni_3Ta, L + Ni_3Ta, Ni_3Ta + L, Ni_2Ta + L, L + NiTa, L + NiTa_2, L + Ta, Ni + Ni_8Ta, Ni_8Ta, Ni_8Ta + Ni_3Ta, Ni_3Ta, Ni_3Ta + Ni_2Ta, Ni_2Ta, Ni_2Ta + NiTa, NiTa, NiTa + NiTa_2, NiTa_2, NiTa_2 + Ta, Ni, \text{-}Base, Ta, \text{-}Nickel, \text{-}Tantalum, \text{-}Top, L\}$

TABLE III

In order to suggest ways in which the incidence calculus may be used to model not only the topological relationships in phase equilibria, but also thermodynamic relationships, we make the following informal definitions:

f-equilibria* $\equiv$ the incidence set of the *k-face* denoting *f-equilibria*.

$\#$ (*f-equilibria**) $\equiv$ number of phase field labels in *f-equilibria**;

$\#P$ (*f-equilibria**) $\equiv$ number of distinct phase labels in *f-equilibria**.

$\#P^+$(*f-equilibrium*$_1^*$,*f-equilibrium*$_2^*$) $\equiv$ number of phases which appear in going from *f-equilibrium*$_1$ to *f-equilibrium*$_2$.

$\#P^-$(*f-equilibrium*$_1^*$,*f-equilibrium*$_2^*$) $\equiv$ number of phases which disappear in going from *f-equilibrium*$_1$ to *f-equilibrium*$_2$.

$\#V$(*f-equilibria*) $\equiv f$, the degrees of freedom, or variance for *f-equilibria*.

F(*f-equilibria*) $\equiv$ the *k-face* denoting *f-equilibria*. Note that $k \geq f$.

I(*f-equilibria**) $\equiv$ the dual incidence set for *f-equilibria**.

$\#D$(*f-equilibria**) $\equiv$ k, the topological dimension of the *k-face* denoting *f-equilibria**.

Note that $\#V$(*f-equilibria*)$\leq\#D$(*f-equilibria**), e.g., for a binary eutectic e, $\#V(e)=0$ and $\#D(e^*)=1$. All operations except $\#V$ are directly computable from the given incidence set. While $\#V$ is not, it may be calculated by applying Gibb's phase rule.

Let $C\equiv n$ be the number of components in a n-ary iso-baric temperature-composition phase diagram. Then a number of qualitative principles may be expressed in terms of the incidence calculus. For example, we give informal translations of the following:

(1) Gibbs Phase Rule [1,2,13,15]: Gibbs phase rule allows the calculation of $\#V$ by the following:

$$\#V(\textit{f-equilibria}) = C - \#P(\textit{f-equilibria}) + 1$$

(2) Boundary Rule [14]: A phase region *f-equilibrium* is bounded by phase regions *g-equilibria*, $g < f$, whose number of phases is constrained by:

$$\#P(\textit{g-equilibrium}^*) = \#P(\textit{f-equilibrium}^*) \pm (C - \#D(\textit{MEET}(\textit{g-equilibrium}^*, \textit{f-equilibrium}^*))$$

The phase fields i.e., *n-faces* of a n-ary diagram, as a special case, gain or lose at most one phase in passing through a $(n-1)$-*face*:

$$\text{If } \textit{(n-1)-equilibria}^* \equiv \{\textit{n-equilibrium}_1, \textit{n-equilibrium}_2\} \text{ then}$$

$$\#P(\textit{n-equilibrium}_1^*) = \#P(\textit{n-equilibrium}_2^*) \pm 1$$

(3) Contact Rule [15] or Law of Adjoining Phase Regions Rule [2]: This rule constrains the dimensionality of the meet of two *f-equilibria* in terms of the number of phases added and deleted in passing through the meet.

$$F(\textit{f-equilibria}_1 \downarrow \textit{f-equilibria}_2) = \textit{k-face} \text{ if and only if}$$

$$k = n - \#P^-(\textit{f-equilibrium}_1^*, \textit{f-equilibrium}_2^*) - \#P^+(\textit{f-equilibrium}_1^*, \textit{f-equilibrium}_2^*) \geq 0$$

We have been very informal here. To be complete, a discussion of how phase field labels are to be encoded, including external face labels, and precisely how the operations defined above are to be computed must be given.

Hillert, in [13], surveys general topological principles underlying phase diagrams and related methods for giving a qualitative geometric interpretation to thermodynamic equilibria. We suggest that these and other qualitative principles, expressed in terms of operations on incidence sets, provide a computational basis for modeling phase equilibria topology.

6. THE INHERENT SUBSYSTEM INCIDENCE RELATIONS IN A MULTICOMPONENT PHASE DIAGRAM DATA BASE

We envision a relational data base[16,17] in which the individual *f-equilibria* for a given fixed phase diagram become the objects for which various attribute values are stored. Included as attributes are the incidence set, its location in temperature-composition space(coordinates for vertices, parametric functions for edges and surfaces etc.), and other information specific to that *f-equilibria*. This organization reflects our belief that the topological information, i.e., the incidences between the *f-equilibria*, must not only be explicitly represented in a data base, but in fact provide the natural structure upon which to "hang" the metric attributes of individual *f-equilibria*. Such a representation links the ability of the computer to perform qualitative reasoning with quantitative calculations, and constitutes the within diagram or "intra-diagram" data base. In the preceding sections, we have described what we call the intra-diagram incidence calculus. A collection of diagrams represented in this manner potentially constitutes a between diagram or "inter-diagram" data base. Questions of type 5 are then a matter of understanding the natural relationships that exist in this inter-diagram data base. We give a brief overview of these inter-diagram relationships.

Let $[a_1,a_2,\cdots,a_n]$ denote a fixed ordering, called a component sequence , of the n components $a_1,a_2,\cdots,a_n$ making up a n-ary phase diagram. Denote by $[a_n]_i^j$, $0\le i\le j\le n$, the compatible component sequence set consisting of the collection of ordered component sequences in which the n components $a_1,a_2,\cdots,a_n$ are taken $0\le i, i+1,\cdots,j-1, j\le n$ at a time. Further, denote by $P_i^j[a_n]$ the collection of phase diagrams, each member of which corresponds to a unique component sequence in $[a_n]_i^j$. Note that the collection $P_i^j[a_n]$ contains $\sum_{k=i}^{j}\binom{n}{k}$ distinct phase diagrams. In case $i=j=n$, $[a_n]_n^n$, abbreviated to $[a_n]$, there is a single n-ary phase diagram, again abbreviated to $P[a_n]$, and even more briefly as P, corresponding to the single component sequence $[a_1,a_2,\cdots,a_n]$.

More specifically, let $[e_1,e_2,\cdots,e_{max}]$ denote a fixed component sequence for the *max* elements of potential interest in a phase diagram data base, and let $U[e_{max}]$ denote the max-ary "universal" phase diagram on these *max* components. Then all phase diagrams P and Q of potential interest may be thought of as subsystems of U, or to be more precise, members of $U_0^{max}[e_1,e_2,\cdots,e_{max}]$.

If $[a_n]$ and $[b_m]$ are two component sequences, both members of $[e_{max}]_0^{max}$, we say $[a_n]$ is an n-ary sub-component sequence of $[b_m]$ if and only if for $n\le m$, and for all i, $0\le i\le n$, there is a j, $0\le j\le m$, $i\le j$ such that $a_i=b_j$, and denote this relationship by $[a_n]\ll[b_m]$. Note that for component sequence $[a_n]$, the corresponding phase diagram $P[a_n]$, has n, (n-1)-ary subcomponent sequences, each of which correspond to a phase diagram in the collection $P_{n-1}^{n-1}[a_n]$. Further, if $P[a_p]$ and $Q[b_q]$ are p-ary and q-ary phase diagrams respectively, for which $[a_p]$ is a sub-component sequence of $[b_q]$ we define the phase diagram subsystem relation $\ll$ which may exist between them as:

$$P[a_p]\ll Q[b_q] \text{ if and only if } \begin{cases}[a_p]\ll[b_q]\\ [a_p]\ll[e_{max}]\\ [b_q]\ll[e_{max}]\end{cases}$$

Hence, for all phase diagrams P of potential interest, $P\ll U$. However, given two arbitrary subsystems P and Q of U, if both contain components not contained in the other, then neither $P\ll Q$ or $Q\ll P$, and hence the relation $\ll$ induces a partial order on the elements of $U_0^{max}[e_{max}]$, i.e., the subsystems of U. In analogy with the equilibria join $\uparrow$ and meet $\downarrow$ for *k-faces*, we define the subsystem join $\uparrow\uparrow$ and meet $\downarrow\downarrow$ of any two subsystems P and Q of the universal phase diagram U:

$$P[a_p]\uparrow\uparrow Q[b_q]=R[c_r] \text{ if and only if } \begin{cases}r\ge max(p,q)\\ R[c_r]\gg P[a_p]\\ R[c_r]\gg Q[b_q]\\ r \text{ is minimum}\end{cases}$$

$$P[a_p]\downarrow\downarrow Q[b_q]=R[c_r] \text{ if and only if } \begin{cases}r\le min(p,q)\\ R[c_r]\ll P[a_p]\\ R[c_r]\ll Q[b_q]\\ r \text{ is maximum}\end{cases}$$

The subsystem relation $<<$ along with the join $\uparrow\uparrow$ and meet $\downarrow\downarrow$ operations define a subsystem incidence lattice in which the universal system $U_n^n[e_{max}] \equiv U$ is the LUB and the 0-ary system $U_0^0[e_{max}] \equiv 0[e_{max}]$ is the GLB. It is this mathematical lattice of phase diagrams that we have denoted by $U_0^{max}[e_{max}]$, and note that its structure models the natural relationships which exist between the various subsystem phase diagrams of the universal phase diagram $U[e_1, e_2, \cdots, e_{max}]$. Hence, the intrinsic incidence relationships inherent in the inter-diagram data base $U_0^{max}[e_{max}]$ are modeled by the same structures used in modeling the *f-equilibria* intra-diagram data base. The n-ary transition equilibria information is in the interior of the *n-face*, while the *(n-1)-faces*, *(n-2)-faces*, $\cdots$, *0-faces* contain the (n-1)-ary, (n-2)-ary, ... , 0-ary subsystem equilibria respectively. This induces an inter-diagram incidence lattice defined on the collection of individual intra-diagram incidence lattices. This becomes apparent when we consider the ternary prism shell P[A,B,C].

To pursue this example, refer back to the ternary prism of figure 2. Here the universal diagram $U_3^3[A,B,C]$ is $P[A,B,C]$, and the subsystem lattice $U_0^3[A,B,C]$ consists of $P_3^3[A,B,C] \equiv$LUB, its subsystems $P_2^2[A,B,C] \equiv \{P[A,B], P[B,C], P[C,A]\}$, its subsubsystems $P_1^1[A,B,C] \equiv \{P[A], P[B], P[C]\}$ and $P_0^0[A,B,C] \equiv$LUB. Hence $P[A,B] \uparrow\uparrow P[B,C] = P[A,B,C]$ and $P[A,B] \downarrow\downarrow P[B,C] = P[B]$ for example. It is this incidence lattice that the incidence calculus $T_{P[A,B,C]}$ given in table I models since in fact none of the faces contain interior equilibria. This is just the relationship between the ternary of figure 1 and the corresponding barycentric coordinate system shell of figure 2. Each of the three subsytem faces contribute a unique label to that subsystem's label set, so that the three binary incidence calculii may be easily distinguished within the ternary incidence calculus. We call the incidence sets corresponding to this subsystem incidence lattice, the subsystem incidence calculus.

These subsystem relations are of course well known, but we have elaborated them here because we see them as an important consideration in the architectual design of a multicomponent phase diagram data base. While the intra-diagram incidence lattice varies from diagram to diagram, the subsystem inter-diagram incidence lattice is fixed and provides a framework upon which to hang shared phase equilibria information in a consistent manner.

The incidence calculus for this framework is relatively straight forward to calculate for an arbitrary number of components n. For example, figure 7 is the four component, i.e., quaternary, analogue of figure 2 and the calculated subsystem incidence calculus for it is given in table IV. Note that the *4-face* is really the LUB, but for consistency we have included the (redundant) empty set {} corresponding to the interior complex of *i-faces*, of which there is only the single *4-face* α.

In general, for a n-ary phase diagram within a n component barycentric coordinate system with n-1 axes and one additional linear axis, e.g., temperature, the number of *i-faces*, for $i = 0, 1, \cdots, n$ is easily calculated. Let F_i^n be the set of *i-faces* of dimension i, and denote by #(S) the number of elements in the set S. Then the number of *i-faces* of dimension i is given by:

$$\#(F_i^n) = \begin{cases} 2n & i=0 \quad \text{(vertices)} \\ 2\binom{n}{i+1} + \binom{n}{i} & 0<i<n \\ 2 & i=n \quad \text{(interior and exterior)} \end{cases}$$

For example, the number of *(n-1)-faces* of a n-ary system is obtained by setting i to $n-1$, and is given by $2\binom{n}{n} + \binom{n}{n-1} = 2+n$, which corresponds to the n subsystem faces and the two truncated faces of the temperature scale. The term $\binom{n}{i}$ is the number of (i-ary)-subsystems in F_i^n, denoted by S_i^n, while the term $2\binom{n}{i+1}$ is the number of "end" *i-faces* created by the upper and lower temperature range truncations.

Given the existence of the incidences between the subsystems of a multicomponent phase diagram data base, as outlined above, we next briefly outline what is meant by algorithmically computing the meet and join of two incidence lattices corresponding to elements of $U_0^{max}[e_{max}]$.

7. AN OPERATIONAL CALCULUS FOR A MULTICOMPONENT PHASE DIAGRAM DATA BASE

In particular we are interested in facilitating a "bootstrapping" process whereby the lower order systems in conjunction with the application of the generic rules of thermodynamics, as well as their application to specific systems, and including laboratory data, are used to build a multicomponent phase

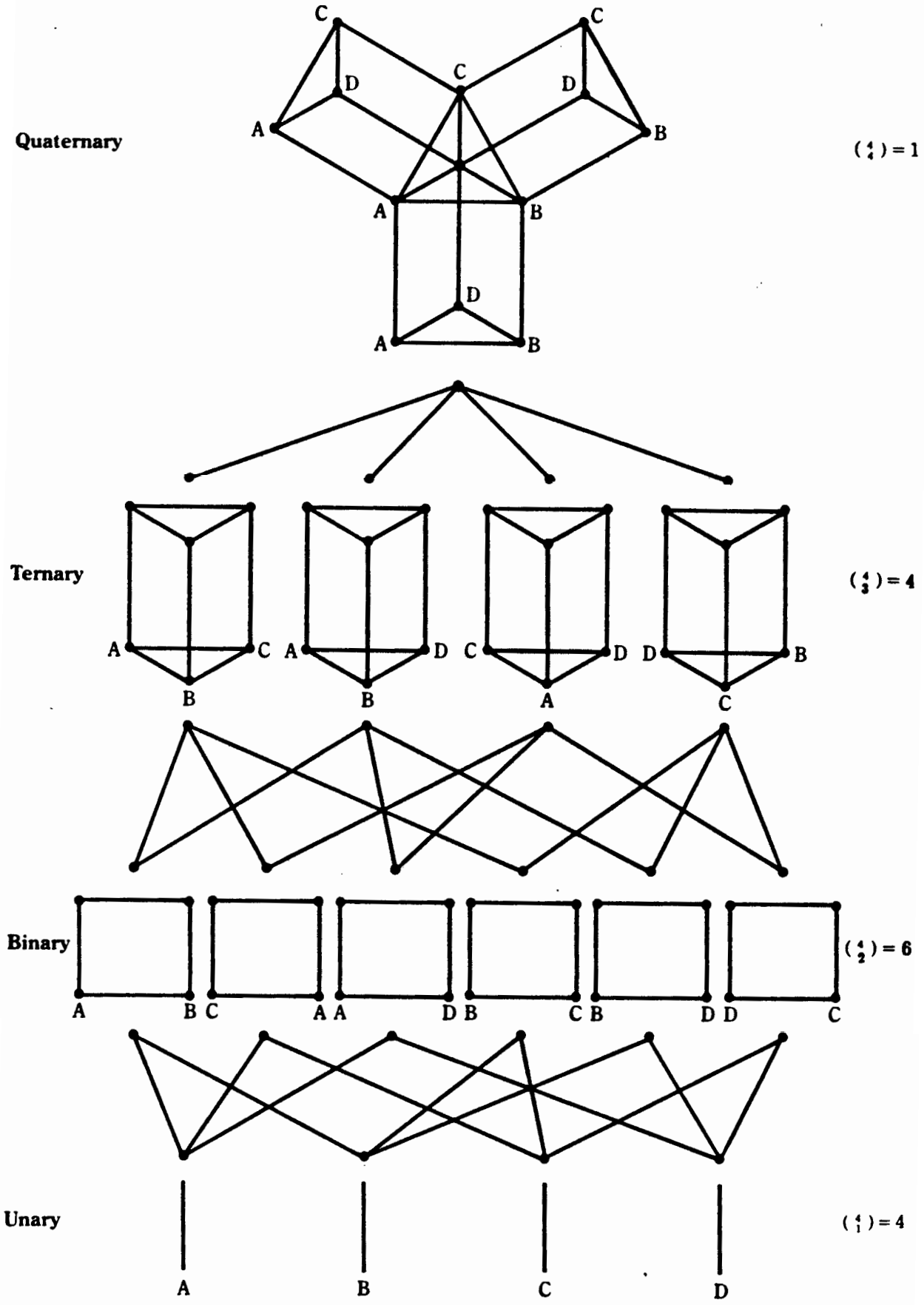

Figure 7. A schematic of a quaternary "coordinate shell" and its decomposition into faces of decreasing dimension. Except for the truncated temperature base and liquidus faces (not shown), these faces correspond to the subsystems of decreasing dimension from which it was composed. Its incidence calculus is given in table IV.

Quaternary A-B-C-D Subsystem Incidence Calculus				
K	Index	Vertex Set	Incidence Set	Subsystem
0-Faces	1	$\{v_1\}$	{-*Base*,α,*A-B-D*,*A-B-C*,*C-A-D*}	
	2	$\{v_2\}$	{-*Base*,α,*A-B-D*,*A-B-C*,*B-C-D*}	
	3	$\{v_3\}$	{-*Base*,α,*A-B-C*,*C-A-D*,*B-C-D*}	
	4	$\{v_4\}$	{-*Base*,α,*A-B-D*,*C-A-D*,*B-C-D*}	
	5	$\{v_5\}$	{α,-*Top*,*A-B-D*,*A-B-C*,*C-A-D*}	
	6	$\{v_6\}$	{α,-*Top*,*A-B-D*,*A-B-C*,*B-C-D*}	
	7	$\{v_7\}$	{α,-*Top*,*A-B-C*,*C-A-D*,*B-C-D*}	
	8	$\{v_8\}$	{α,-*Top*,*A-B-D*,*C-A-D*,*B-C-D*}	
1-Faces	1	$\{v_1,v_2\}$	{-*Base*,α,*A-B-D*,*A-B-C*}	
	2	$\{v_1,v_3\}$	{-*Base*,α,*A-B-C*,*C-A-D*}	
	3	$\{v_1,v_4\}$	{-*Base*,α,*A-B-D*,*C-A-D*}	
	4	$\{v_1,v_5\}$	{α,*A-B-D*,*A-B-C*,*C-A-D*}	Unary A
	5	$\{v_2,v_3\}$	{-*Base*,α,*A-B-C*,*B-C-D*}	
	6	$\{v_2,v_4\}$	{-*Base*,α,*A-B-D*,*B-C-D*}	
	7	$\{v_2,v_6\}$	{α,*A-B-D*,*A-B-C*,*B-C-D*}	Unary B
	8	$\{v_3,v_4\}$	{-*Base*,α,*C-A-D*,*B-C-D*}	
	9	$\{v_3,v_7\}$	{α,*A-B-C*,*C-A-D*,*B-C-D*}	Unary C
	10	$\{v_4,v_8\}$	{α,*A-B-D*,*C-A-D*,*B-C-D*}	Unary D
	11	$\{v_5,v_6\}$	{α,-*Top*,*A-B-D*,*A-B-C*}	
	12	$\{v_5,v_7\}$	{α,-*Top*,*A-B-C*,*C-A-D*}	
	13	$\{v_5,v_8\}$	{α,-*Top*,*A-B-D*,*C-A-D*}	
	14	$\{v_6,v_7\}$	{α,-*Top*,*A-B-C*,*B-C-D*}	
	15	$\{v_6,v_8\}$	{α,-*Top*,*A-B-D*,*B-C-D*}	
	16	$\{v_7,v_8\}$	{α,-*Top*,*C-A-D*,*B-C-D*}	
2-Faces	1	$\{v_1,v_2,v_5,v_6\}$	{α,*A-B-D*,*A-B-C*}	Binary A-B
	2	$\{v_1,v_3,v_5,v_7\}$	{α,*A-B-C*,*C-A-D*}	Binary A-C
	3	$\{v_1,v_4,v_5,v_8\}$	{α,*A-B-D*,*C-A-D*}	Binary A-D
	4	$\{v_2,v_3,v_6,v_7\}$	{α,*A-B-C*,*B-C-D*}	Binary B-C
	5	$\{v_2,v_4,v_6,v_8\}$	{α,*A-B-D*,*B-C-D*}	Binary B-D
	6	$\{v_3,v_4,v_7,v_8\}$	{α,*C-A-D*,*B-C-D*}	Binary C-D
	7	$\{v_1,v_2,v_3\}$	{-*Base*,α,*A-B-C*}	
	8	$\{v_1,v_2,v_4\}$	{-*Base*,α,*A-B-D*}	
	9	$\{v_1,v_3,v_4\}$	{-*Base*,α,*C-A-D*}	
	10	$\{v_2,v_3,v_4\}$	{-*Base*,α,*B-C-D*}	
	11	$\{v_5,v_6,v_7\}$	{α,-*Top*,*A-B-C*}	
	12	$\{v_5,v_6,v_8\}$	{α,-*Top*,*A-B-D*}	
	13	$\{v_5,v_7,v_8\}$	{α,-*Top*,*C-A-D*}	
	14	$\{v_6,v_7,v_8\}$	{α,-*Top*,*B-C-D*}	
3-Faces	1	$\{v_1,v_2,v_3,v_5,v_6,v_7\}$	{α,*A-B-C*}	Ternary A-B-C
	2	$\{v_1,v_2,v_4,v_5,v_6,v_8\}$	{α,*A-B-D*}	Ternary A-B-D
	3	$\{v_1,v_3,v_4,v_5,v_7,v_8\}$	{α,*C-A-D*}	Ternary C-A-D
	4	$\{v_2,v_3,v_4,v_6,v_7,v_8\}$	{α,*B-C-D*}	Ternary B-C-D
	5	$\{v_1,v_2,v_3,v_4\}$	{-*Base*,α}	
	6	$\{v_5,v_6,v_7,v_8\}$	{α,-*Top*}	
4-Faces	1	$\{v_1,v_2,v_3,v_4,v_5,v_6,v_7,v_8\}$	{α}	Quaternary
GLB	1	{}	{-*Base*,*A-B-C*,α,-*Top*,*A-B-D*,*C-A-D*,*B-C-D*}	
LUB	1	$\{v_i\}_{i=1,8}$	{}	

TABLE IV

diagram data base. The role of the subsystem incidence calculus is that of an operational representation, amenable to computer manipulation, and acts as a complement to thermodynamic modeling by providing the superstructure upon which to hang the metric attributes such modeling generates.

For each element $P[a_n]$ of $U_0^{\max}[e_{\max}]$ there is an intra-diagram incidence calculus $T_{P[a_n]}$. This collection of incidence calculi, corresponding to the individual calculi of elements in $U_0^{\max}[e_{\max}]$, we call the inter-diagram incidence calculus, and denote it by $D^{U_0^{\max}[e_{\max}]}$. The abstract partial order between the elements of $U_0^{\max}[e_{\max}]$ may be expressed operationally in terms of their individual incidence calculi as

$$P[a_p] << Q[b_q] \text{ if and only if } T_{P[a_p]} \subset_T T_{Q[b_q]},$$

where $\subset_T$ is a suitably defined sub-lattice relationship defined on the incidence calculi. For example, given the incidence sets for $T_{P[A,B,C]}$, (which strictly speaking is a subsystem incidence calculus, but the techniques are the same), we can readily identify the subcalculus for $T_{P[A,B]}$ as consisting of those incidence sets containing the label A-B, e.g., $T_{P[A,B]} \approx \{s \in T_{P[A,B,C]} \mid A\text{-}B \in s\}$. These are $\bar{\alpha}^*, v_1^*, v_2^*, v_4^*, v_5^*, e_{12}^*, e_{14}^*, e_{25}^*$ and e_{24}^*. However, in order for the set theoretic operations modeling $<$, $\uparrow$ and $\downarrow$ to work, we must remove all labels A-B, and replace labels of the form C-A with A and A-B with B. The empty set $\{\}$=GLB and the set containing all the resulting labels, the LUB, must also be added.

The computation associated with the meet $\downarrow\downarrow$ is motivated by wanting to find the incidence calculus for the subsystem of highest dimension common to several systems.

Given $P[a_p]$, $Q[b_q]$ and $R[C_r]$ such that

$$P[a_p] \downarrow\downarrow Q[b_q] = R[C_r]$$

then clearly we want

$$T_{P[a_p]} \cap_T T_{Q[b_q]} = T_{R[C_r]},$$

where again $\cap_T$ is a suitably defined "intersection" on incidence calculi. Again, using $T_{P[A,B,C]}$ as an example, if we are given $P[A,B] \downarrow\downarrow Q[B,C] = R[B]$, then we are interested in defining $\cap_T$ so that $T_{P[A,B]} \cap_T T_{Q[B,C]} = T_{R[B]}$. This will be true if we define it as

$$T_{P[A,B]} \cap_T T_{Q[B,C]} = \{s \mid s \in T_{P[A,B]} \text{ and } s \in T_{Q[B,C]}\}$$

suitably relabeled with the LUB and GLB added.

The much more interesting possibility is that of being given the incidence calculi for the n (n-1)-ary systems of $P_{n-1}^{n-1}[a_n]$, with the objective of "bootstrapping" up to the minimally induced incidence calculus containing the given incidence calculi as subcalculi. Let the n elements of $P_{n-1}^{n-1}[a_n]$ be denoted by $P_i[a_n]$, and their corresponding incidence calculi by $T_i[a_n]$, $i=1,n$. By definition $P_i[a_n] \uparrow\uparrow P_j[a_n] = P[a_n]$, $1 \le i,j \le n$, $i \ne j$, and we are interested in "computing" $T_{P[a_n]}$. Again we are interested in defining a "union" operation $\cup_T$ such that

$$T_1[a_n] \cup_T T_2[a_n] \cup_T \cdots \cup_T T_n[a_n] \equiv T_{P[a_n]}$$

As an example, figure 8 consists of a generic ternary $P[A,B,C]$ made up of an isomorphous subsytem $P[A,B]$, and two eutectic subsystems $P[B,C]$ and $P[C,A]$. Hence,

$$P[A,B,C] = P[A,B] \uparrow\uparrow P[B,C] \uparrow\uparrow P[C,A]$$

and we want to find a minimally induced incidence calculus $T_{P[A,B,C]}$ so that

$$T_{P[A,B,C]} = T_{P[A,B]} \cup_T T_{P[B,C]} \cup_T T_{P[C,A]}$$

In this case the two eutectics must extend to form an "eutectic trough", but no internal vertex (ternary eutectic) is required, as say would be the case if all three binary subsytems were of the eutectic type. Hence only sharing of unary subsystem vertices and reinterpreting *2-face* labels (phase fields) as *3-face* labels (phase volumes) must be done. One of (in general there will be more than one) the resulting minimally induced incidence calculi, $T_{P[A,B,C]}$, (which includes an hypothesized three phase field $L+\alpha+\beta$), is depicted in table V.

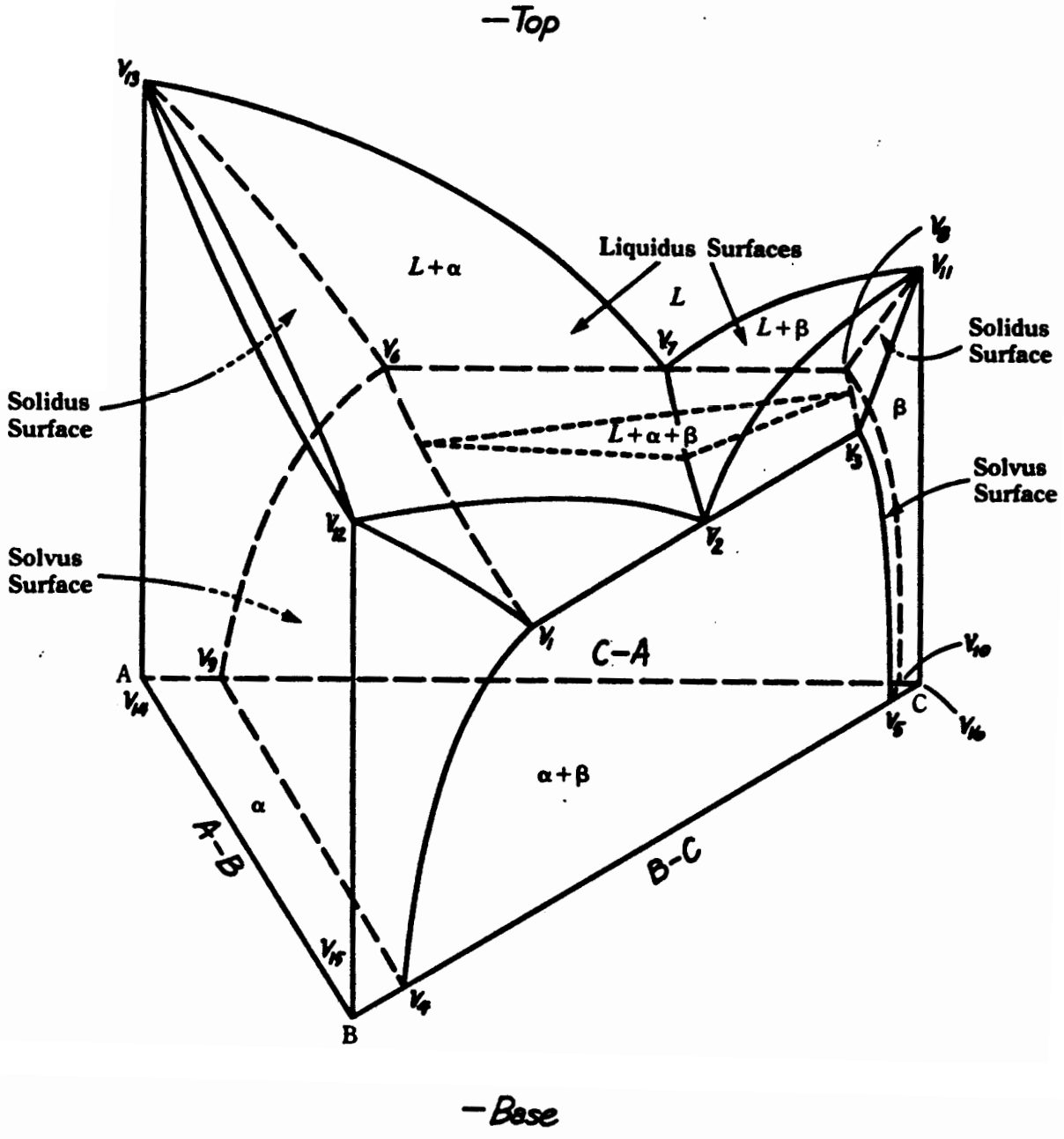

Figure 8. A schematic of a ternary made from two eutectic and one isomorphous system. Its incidence calculus is given in table V, and is potentially calculatable from the three incidence calculi of the subsystems composing it.

TABLE V: Generic Eutectic-Eutectic-Isomorphous Ternary

K	Index	Vertex Set	Incidence Set
Vertices	1	$\{v_1\}$	$\{B\text{-}C,\alpha,\alpha+\beta,L+\alpha,L+\alpha+\beta\}$
	2	$\{v_2\}$	$\{B\text{-}C,L,L+\beta,\alpha+\beta,L+\alpha,L+\alpha+\beta\}$
	3	$\{v_3\}$	$\{B\text{-}C,\beta,L+\beta,\alpha+\beta,L+\alpha+\beta\}$
	4	$\{v_4\}$	$\{B\text{-}C,\alpha,\alpha+\beta,\text{-}Base\}$
	5	$\{v_5\}$	$\{B\text{-}C,\beta,\alpha+\beta,\text{-}Base\}$
	6	$\{v_6\}$	$\{C\text{-}A,\alpha,\alpha+\beta,L+\alpha,L+\alpha+\beta\}$
	7	$\{v_7\}$	$\{C\text{-}A,L,L+\beta,\alpha+\beta,L+\alpha,L+\alpha+\beta\}$
	8	$\{v_8\}$	$\{C\text{-}A,\beta,L+\beta,\alpha+\beta,L+\alpha+\beta\}$
	9	$\{v_9\}$	$\{C\text{-}A,\alpha,\alpha+\beta,\text{-}Base\}$
	10	$\{v_{10}\}$	$\{C\text{-}A,\beta,\alpha+\beta,\text{-}Base\}$
	11	$\{v_{11}\}$	$\{B\text{-}C,C\text{-}A,\beta,L+\beta,L,\text{-}Top\}$
	12	$\{v_{12}\}$	$\{A\text{-}B,B\text{-}C,L+\alpha,\alpha,L,\text{-}Top\}$
	13	$\{v_{13}\}$	$\{A\text{-}B,C\text{-}A,L+\alpha,\alpha,L,\text{-}Top\}$
	14	$\{v_{14}\}$	$\{A\text{-}B,C\text{-}A,\alpha,\text{-}Base\}$
	15	$\{v_{15}\}$	$\{A\text{-}B,B\text{-}C,\text{-}Base,\alpha\}$
	16	$\{v_{16}\}$	$\{\text{-}Base,C\text{-}A,B\text{-}C,\beta\}$
Edges	1	$\{v_1,v_2\}$	$\{B\text{-}C,\alpha+\beta,L+\alpha,L+\alpha+\beta\}$
	2	$\{v_1,v_4\}$	$\{B\text{-}C,\alpha,\alpha+\beta\}$
	3	$\{v_1,v_6\}$	$\{\alpha,\alpha+\beta,L+\alpha,L+\alpha+\beta\}$
	4	$\{v_1,v_{12}\}$	$\{B\text{-}C,\alpha,L+\alpha\}$
	5	$\{v_2,v_3\}$	$\{B\text{-}C,L+\beta,\alpha+\beta,L+\alpha+\beta\}$
	6	$\{v_2,v_7\}$	$\{L,L+\beta,\alpha+\beta,L+\alpha,L+\alpha+\beta\}$
	7	$\{v_2,v_{11}\}$	$\{B\text{-}C,L,L+\beta\}$
	8	$\{v_2,v_{12}\}$	$\{B\text{-}C,L,L+\alpha\}$
	9	$\{v_3,v_5\}$	$\{B\text{-}C,\beta,\alpha+\beta\}$
	10	$\{v_3,v_8\}$	$\{\beta,L+\beta,\alpha+\beta,L+\alpha+\beta\}$
	11	$\{v_3,v_{11}\}$	$\{B\text{-}C,\beta,L+\beta\}$
	12	$\{v_4,v_5\}$	$\{B\text{-}C,\alpha+\beta,\text{-}Base\}$
	13	$\{v_4,v_9\}$	$\{\alpha,\alpha+\beta,\text{-}Base\}$
	14	$\{v_4,v_{15}\}$	$\{B\text{-}C,\alpha,\text{-}Base\}$
	15	$\{v_5,v_{10}\}$	$\{\beta,\alpha+\beta,\text{-}Base\}$
	16	$\{v_5,v_{16}\}$	$\{B\text{-}C,\beta,\text{-}Base\}$
	17	$\{v_6,v_7\}$	$\{C\text{-}A,\alpha+\beta,L+\alpha,L+\alpha+\beta\}$
	18	$\{v_6,v_9\}$	$\{C\text{-}A,\alpha,\alpha+\beta\}$
	19	$\{v_6,v_{13}\}$	$\{C\text{-}A,\alpha,L+\alpha\}$
	20	$\{v_7,v_8\}$	$\{C\text{-}A,L+\beta,\alpha+\beta,L+\alpha+\beta\}$
	21	$\{v_7,v_{11}\}$	$\{C\text{-}A,L,L+\beta\}$
	22	$\{v_7,v_{13}\}$	$\{C\text{-}A,L,L+\alpha\}$
	23	$\{v_8,v_{10}\}$	$\{C\text{-}A,\beta,\alpha+\beta\}$
	24	$\{v_8,v_{11}\}$	$\{C\text{-}A,\beta,L+\beta\}$
	25	$\{v_9,v_{10}\}$	$\{C\text{-}A,\alpha+\beta,\text{-}Base\}$
	26	$\{v_9,v_{14}\}$	$\{C\text{-}A,\alpha,\text{-}Base\}$
	27	$\{v_{10},v_{16}\}$	$\{C\text{-}A,\beta,\text{-}Base\}$
	28	$\{v_{11},v_{12}\}$	$\{B\text{-}C,L,\text{-}Top\}$
	29	$\{v_{11},v_{13}\}$	$\{C\text{-}A,L,\text{-}Top\}$
	30	$\{v_{11},v_{16}\}$	$\{B\text{-}C,C\text{-}A,\beta\}$
	31	$\{v_{12},v_{13}\}$	$\{A\text{-}B,L+\alpha,\alpha,L,\text{-}Top\}$
	32	$\{v_{12},v_{15}\}$	$\{A\text{-}B,B\text{-}C,\alpha\}$
	33	$\{v_{13},v_{14}\}$	$\{A\text{-}B,C\text{-}A,\alpha\}$
	34	$\{v_{14},v_{15}\}$	$\{A\text{-}B,\alpha,\text{-}Base\}$
Faces	1	$\{v_1,v_2,v_3,v_6,v_7,v_8\}$	$\{\alpha+\beta,L+\alpha+\beta\}$
	2	$\{v_1,v_2,v_3,v_4,v_5\}$	$\{B\text{-}C,\alpha+\beta\}$
	3	$\{v_6,v_7,v_8,v_9,v_{10}\}$	$\{C\text{-}A,\alpha+\beta\}$
	4	$\{v_1,v_4,v_6,v_9\}$	$\{\alpha,\alpha+\beta\}$
	5	$\{v_1,v_4,v_{12},v_{15}\}$	$\{B\text{-}C,\alpha\}$

TABLE V: Generic Eutectic-Eutectic-Isomorphous Ternary			
K	Index	Vertex Set	Incidence Set
Faces	6	$\{v_1,v_6,v_{12},v_{13}\}$	$\{\alpha,L+\alpha\}$
	7	$\{v_2,v_7,v_{12},v_{13}\}$	$\{L,L+\alpha\}$
	8	$\{v_3,v_5,v_8,v_{10}\}$	$\{\beta,\alpha+\beta\}$
	9	$\{v_3,v_5,v_{11},v_{16}\}$	$\{B\text{-}C,\beta\}$
	10	$\{v_4,v_5,v_9,v_{10}\}$	$\{\alpha+\beta,\text{-}Base\}$
	11	$\{v_4,v_5,v_{15},v_{16}\}$	$\{B\text{-}C,\text{-}Base\}$
	12	$\{v_4,v_9,v_{14},v_{15}\}$	$\{\alpha,\text{-}Base\}$
	13	$\{v_6,v_9,v_{13},v_{14}\}$	$\{C\text{-}A,\alpha\}$
	14	$\{v_8,v_{10},v_{11},v_{16}\}$	$\{C\text{-}A,\beta\}$
	15	$\{v_9,v_{10},v_{14},v_{16}\}$	$\{C\text{-}A,\text{-}Base\}$
	16	$\{v_{12},v_{13},v_{14},v_{15}\}$	$\{A\text{-}B,\alpha\}$
	17	$\{v_1,v_2,v_{12}\}$	$\{B\text{-}C,L+\alpha\}$
	18	$\{v_2,v_3,v_{11}\}$	$\{B\text{-}C,L+\beta\}$
	19	$\{v_2,v_7,v_{11}\}$	$\{L,L+\beta\}$
	20	$\{v_2,v_{11},v_{12}\}$	$\{B\text{-}C,L\}$
	21	$\{v_3,v_8,v_{11}\}$	$\{\beta,L+\beta\}$
	22	$\{v_5,v_{10},v_{16}\}$	$\{\beta,\text{-}Base\}$
	23	$\{v_6,v_7,v_{13}\}$	$\{C\text{-}A,L+\alpha\}$
	24	$\{v_7,v_8,v_{11}\}$	$\{C\text{-}A,L+\beta\}$
	25	$\{v_7,v_{11},v_{13}\}$	$\{C\text{-}A,L\}$
	26	$\{v_{11},v_{12},v_{13}\}$	$\{L,\text{-}Top\}$
Volumes	1	$\{v_1,v_2,v_3,v_4,v_5,v_6,v_7,v_8,v_9,v_{10}\}$	$\{\alpha+\beta\}$
	2	$\{v_1,v_4,v_6,v_9,v_{12},v_{13},v_{14},v_{15}\}$	$\{\alpha\}$
	3	$\{v_1,v_2,v_6,v_7,v_{12},v_{13}\}$	$\{L+\alpha\}$
	4	$\{v_3,v_5,v_8,v_{10},v_{11},v_{16}\}$	$\{\beta\}$
	5	$\{v_2,v_3,v_7,v_8,v_{11}\}$	$\{L+\beta\}$
	6	$\{v_2,v_7,v_{11},v_{12},v_{13}\}$	$\{L\}$
GLB	1	$\{\}$	$\{L+\alpha+\beta,\alpha+\beta,L+\beta,L+\alpha,L,\text{-}Top,A\text{-}B,\alpha,\text{-}Base,C\text{-}A,B\text{-}C,\beta\}$
LUB	1	$\{v_i\}_{i=1,16}$	$\{\}$
Special †	1	$\{v_1,v_2,v_6,v_7\}$	$\{\alpha+\beta,L+\alpha,L+\alpha+\beta\}$
	2	$\{v_2,v_3,v_7,v_8\}$	$\{L+\beta,\alpha+\beta,L+\alpha+\beta\}$

TABLE V

To make sure there is no misunderstanding in what we are outlining, it should be emphasized that in suggesting a method for hypothesizing a minimal topology we are in no way modeling or predicting a-priori what the actual higher dimensional phase diagram topology is, but rather only providing a formalism for enumerating the simplest possibile topological extrapolations consistent with the subsystem topologies. It is minimal in the sense that it is a subset of the actual topology, since for example, the existence of a ternary miscibility gap or ternary compound can not be known from just the binary subsytems. Additionally, qualitative thermodynamic rules, expressed in terms of incidence calculus transformations, potentially provide a formal way of decreasing the number of possible topologies even further.

8. FUTURE RESEARCH

In practice, the preceeding ideas must be tempered by the fact that the number of systems we are interested in far exceeds both available laboratory equilibrium data and current thermodynamic modeling techniques. Current emphasis of the latter is on computing what we have called *f-equilibria* metric attributes. As a supplement to modeling these numeric attributes, we have presented a method of representing the qualitative topological relationships, and have suggested the possibility for qualitative modeling of *f-equilibria*.

†These must be interpreted as a volume $\{L+\alpha+\beta\}$, and two faces, $\{L+\alpha+\beta,L+\alpha\}$ and $\{L+\alpha+\beta,L+\beta\}$. See end of Section 5 for an explanation.

The incidence calculus provides a method for characterizing individual phase diagram topology. In itself however, it does not provide a method for characterizing the topology for the entire class of, say binary, phase diagrams. This is done, for example, in [18], where the quantitative modeling of what we have called the metric attributes is worked out as a mathematical topology. In the previous section we have suggested the possibility of algorithmically finding the minimally induced calculus given all subsystem calculi through the application of qualitative thermodynamic rules. These rules, however, must be represented in a manner amenable to computer manipulation. Thermodynamic modeling seems a formidable problem without some method for taking advantage of the qualitative principles given in, for example[13,15], and translated into transformations on incidence calculi or some similiar purely qualitative medium. To this end, we outline one technique future research might take. We express these ideas in terms of the goal of a characterization of binary phase diagrams.

As with the incidence lattice, we treat the topological elements and their incidences. A (binary) phase diagram is then a graph consisting of nodes and connecting edges. This subset of topological information we call the phase graph and as a graph its dual[19] is well defined, somthing we call the phase adjacency graph. As noted in a previous section, the incidence calculus for this dual is a by-product of computing the diagram incidence calculus. Alternatively, the phase adjacency graph may be created directly by assigning a labeled node to each phase field of the diagram, and then connecting those nodes by directed edges whose corresponding phase fields are contiguous in the phase diagram. This representation of phase diagram topology was explored by the Soviet Academician N.S. Kurnakov sometime prior to 1961. His ideas were utilized for computer entry of binary diagrams as described in [20], where the dual is called a physico-chemical graph. In [15], they are called topological schemes and are systematically explored using combinatorial enumerations of phases and the contact rule. Other applications of the phase (adjacency) graph include that of providing a means for efficiently searching across a collection of systems for an occurrence of a *f-equilibrium* in which only the phases and their adjacencies are relevant, i.e., a series of sub-graph matches.

We take the view that the three fundamental thermodynamic events represented in phase diagrams as a decreasing function of temperature are the appearance or disappearance of a phase, and the reordering of existing phases, called a formation equilibria, decomposition equilibria and transition equilibria respectively in [21]. In the binary case the formation and decomposition equilibria correspond to the peritectic and eutectic invariant equilibria reactions respectively. A (binary) phase diagram "composed" of several such invariant equilibria, or "reactions", say formation and decomposition equilibria for example, will contain three reaction "interaction" types: peritectic-peritectic, eutectic-eutectic and peritectic-eutectic. Each such interaction may have several "solutions", i.e., side by side, one above the other, etc. We define the invariant equilibria co-articulation problem as that of determining the rules concerned with how two invariant equilibria, each expressed as a schematic in the form of an invariant equilibria adjacency graph , link up. Knowing these rules would make possible the algorithmic completion of the topology of an hypothesized phase diagram from a set of hypothesized invariant equilibria. Gibbs phase rule, the boundary rule, the contact rule and other qualitative thermodynamic constraints clearly limit the possible phase orderings, and this, coupled with the algorithm described in this paper, would allow the calculation of the remaining intermediate dimensioned equilibria. We are suggesting that such rules, explicitly stored in the computer as graph/incidence calculus transformation rules and used in conjunction with thermodynamic modeling, would provide a more complete representation of thermodynamic knowledge then is currently being used in modeling efforts.

A potentially useful technique for dealing with thermodynamic rules concerned with transformations on phase adjacency graphs is that of treating these rules as a generative grammar[22,23,24]. A large literature exists explicitly dealing with grammars defined on graphs (See [25], for example.), as well as computer algorithms for dealing with them.

One of the underlying assumptions of such a generative grammar approach is that we are interested in characterizing the topology of an infinite class of potential phase diagrams, only a finite subset of which have actually occurred in nature. This is analogous to what a grammarian does when he attempts to characterize English by a grammar: He hypothesizes an infinite set of potential utterances to characterize, and not just the finite set of utterances that have actually occurred. Such a characterization may be approached simultaneously from two directions: From below with a too restrictive grammar, and from above with a grammar not restrictive enough. Higher order systems would require a more generalized graph grammar formalism, based on for example, hypergraphs[26].

9. SUMMARY

We have informally presented the idea of representing the topological decomposition of a phase diagram as a lattice in such a way as to make questions of a topological nature answerable via set theoretic operations in a calculus modeling that lattice. Its potential advantages are:

(1) Entering for each invariant point, the phases which are incident on that point, or equivalently, for each phase field, the invariant points in which that phase field participates, provides a single unified method for entering and representing phase diagram topology with an arbitrary number of components.

(2) A majority of the topological elements making up a phase diagram, along with their incidences, may be calculated via the algorithm we have presented. The Schlaefli identity, applied to the totality of these elements, provides a method for insuring that a given set of v_i"s describe a topologically consistent diagram.

(3) For a n-ary system, the n (n-1)-ary subsystems contain most of the vertices. Hence knowing the calculus for these n subsystems provides most of the information for the v_i"s needed for the n-ary system, thus providing a "bootstrapping procedure". We have also suggested the possibility of developing a formal model of this process amenable to computer implementation.

(4) The subsystem incidence calculus provides a natural architecture around which to design a multicomponent data base in which the lower order systems provide a single consistent source of data for the higher order systems.

Motivated by design considerations for a computerized phase diagram data base, a description of the inter-diagram relations existing between phase diagrams was given in terms which relate them in a natural way to the intra-diagram equilibria topological relationships.

As an adjunct to quantitative thermodynamic modeling, we have speculated that discrete qualitative topological models, based on incidence calculus transformations and driven by generative graph grammar models, might provide new research techniques.

ACKNOWLEDGMENTS

John Simmons and Lydon Swartzendruber provided the seed idea from which the incidence calculus evolved. The author would like to thank John Cuthill and Rodney Elliott for teaching him about phase diagrams, and Larry Bennett and Russell Kirsch for their continuing encouragement. Sam Coriell, Dave Gilsinn, Tony Gualtieri, Dave Neumann and Ed Paul provided a number of useful comments and corrections for an earlier draft. Dan Kahan provided the phase diagrams used in figures 5 and 6.

REFERENCES

[1] F. N. Rhines,"Phase Diagrams in Metallurgy: Their Development and Application," McGraw-Hill Book Company, New York, 1956.

[2] A. Prince, "Alloy Phase Equilibria," Elsevier Publishing Company, Amsterdam, The Netherlands, 1966.

[3] T. Ichikawa and S. Chang, ed., "1984 IEEE Computer Society Workshop on Visual Languages," December 6-8, 1984 Hiroshima, Japan.

[4] D. Hilbert and S. Cohn-Vossen, "Geometry and the Imagination," Chelsea Publishing Company, New York, 1952.

[5] H. S. M. Coxeter, "Regular Polytopes," 2nd edition, MacMillian and Company, Ltd., New York, 1963, p. 158, p. 166.

[6] G. Gratzer, "Lattice Theory: First Concepts and Distributive Lattices," W. H. Freman and Company, San Francisco, 1971, pp. 1-14.

[7] E. Horowitz and S. Sahni, "Fundamentals of Data Structures," Computer Science Press, 1981, p. 106.

[8] A. L. Loeb, "Space Structures: Their Harmony and Counterpoint," Addison-Wesley Publishing Company, Inc., Reading, Massachusettes, 1976, p. 11-12, p. 39-43.

[9] B. Grunbaum, "Convex Polytopes," Interscience Publishers, New York, 1967, p. 37, 50, 206.

[10] W. H. Burge, "Recursive Techniques in Programming," American Elsevier Publishing Company, Reading, Massachusettes, 1975, p.148.

[11] J. Dutkiewicz and W. Zakulski, "The Cd-Zn (Cadmium-Zinc) System," Bulletin of Alloy Phase Diagrams, 5(1), 1984, p. 30.

[12] A. Nash and P. Nash, "The Ni-Ta Nickel-Tantalum System," Bulletin of Alloy Phase Diagrams, 5(3), 1984, p. 259.

[13] M. Hillert, "Principles of Phase Diagrams," International Metals Reviews, Vol. 30, No. 2, 1985, p. 45.

[14] M. Zhao, "The Theorem of Corresponding Relation Between Neighboring Phase Regions and Their Boundaries in Phase Diagrams(I)," Department of Chemistry, Jilin University, Changchun, People's Republic of China, also, Calphad, 7(3), 1983, p. 185-199.

[15] A. S. Palatnik and A. I. Landau, "Phase Equilibria in Multicomponent Systems," Holt, Rinehart and Winston Inc., New York, 1964.

[16] C.G. Davis, S. Jajodia, P. Ann-Beng Ng and R. Yeh eds., "Entity-Relationship Approach to Software Engineering," North-Holland Publishing Company, Amsterdam, 1983.

[17] Y. C. Lee and K. S. Fu, "Query Languages for Pictorial Database System," in "Natural Language Communication with Pictorial Information Systems," edited by L. Bolc, Springer-Verlag, New York, 1984, pp. 1-142.

[18] Chi-Sing Man, "Material Stability, the Gibbs Conjecture and the First Phase Rule for Substances," Department of Engineering, The University of Manitoba, Winnipeg, 1982.

[19] R. J. Wilson and L.W. Beineke, eds., "Applications of Graph Theory," Academic Press, 1979.

[20] V. S. Shteyn, "Possibilities and Difficulties in Developing an Information Retrieval System for Metals Technology," Russian Metallurgy #2, 1969, p. 111.

[21] N. Kanani and K. Lohberg, "Nomenclature and Geometric Representation of Invariant Phase Equilibria in Multicomponent Systems," Bulletin of Alloy Phase Diagrams, 5(3), 1984, p. 229.

[22] E. Bach, "An Introduction to Transformational Grammars," Holt, Rinehart and Winston, Inc., New York, 1964.

[23] M. Gross and A. Lentin, "Introduction to Formal Grammars," Springer-Verlag, New York, 1970,

[24] L. Nebesky, "Graph Theory and Linguistics," in [19], p. 357.

[25] H. Ehrig, M. Nagel and G. Rozenberg eds., "Graph Grammars and their Application to Computer Science," Lecture Notes in Computer Science No. 153, Springer-Verlag, Berlin, 1983.

[26] C. Berge, "Graphs and Hypergraphs,", North-Holland Publishing Company, Amsterdam, 1973, p. 389.